University of South Bohemia in České Budějovice

Faculty of science

Comparison of photophysiological characteristics of two strains of the cyanobacterium *Trichodesmium* in relation to nitrogen fixation

Master Thesis

Bc. Anežka Terezie Míšková

Supervisor: Meri Eichner, PhD.
Garant from the university: Prof. RNDr. Ondřej Prášil, PhD.

České Budějovice 2022

Míšková, A. T., 2022: Comparison of photophysiological characteristics of two strains of the cyanobacterium *Trichodesmium* in relation to nitrogen fixation. Mgr. Thesis, in English. - 65p., Faculty of Science, University of South Bohemia, České Budějovice, Czech Republic.

Annotation:

Photophysiological characteristics related to nitrogen fixation were studied and compared between two strains (IMS101 and NIBB1067) of the cyanobacterium *Trichodesmium*. To re-evaluate the hypothesis about the relation between nitrogen fixation and phycobilisomes uncoupling, fluorescence lifetime measurements were performed at bulk level using Time-resolved fluorescence spectroscopy and at single-cell resolution using Fluorescence-lifetime imaging microscopy (FLIM). Combination of FLIM with Lugol's stain allowed to directly relate fluorescence lifetime to staining pattern of a commonly used marker of N_2 fixing cells.

Prohlašuji, že jsem autorem této kvalifikační práce a že jsem ji vypracovala pouze s použitím pramenů a literatury uvedených v seznamu použitých zdrojů.

V Českých Budějovicích, 7. prosince 2022

Anežka Terezie Míšková

Acknowledgements:

First of all, I would like to thank my supervisor Meri Eichner for her patient and professional guidance, and above all for her time, willingness and understanding.

Second, I would like to thank David Bína for the measurements and analysis of the Time-resolved fluorescence spectroscopy data. And I also thank him for the valuable advice on the overall content of this work.

Other acknowledgements belong to Davide Basello and Daniel Hadraba from the Institute of Physiology CAS, for their help and guidance in the FLIM measurements.

I would also like to thank all the members of Algatech centre. Namely Rebeca López Adams for the corrections made in this work, Ondřej Prášil for allowing me to work there during my studies, and all my coworkers for their advice, friendly approach and overall pleasant atmosphere.

Last but not least, I would like to thank my family for all the support they gave me during my studies.

Contents

Introduction **1**

1 Photosynthesis **2**
1.1 Marine carbon cycle . . . 2
1.2 Oxygenic photosynthesis . . . 3
1.2.1 Photosynthetic light reactions . . . 3
1.2.2 Photosynthetic dark reactions . . . 6

2 Nitrogen fixation **8**
2.1 Marine nitrogen cycle . . . 8
2.2 N_2 fixation . . . 8

3 Trichodesmium **13**
3.1 Reversible uncoupling of phycobiliproteins . . . 14

4 Fluorescence **16**
4.1 Fluorescence lifetime and its measuring . . . 16
4.1.1 Time-Correlated Single Photon Counting . . . 19

5 Materials and methods **21**
5.1 Culture conditions . . . 21
5.2 Phycobiliprotein extraction . . . 21
5.3 Fluorescence lifetime measurements . . . 22
5.3.1 Time-resolved fluorescence spectroscopy . . . 22
5.3.2 Fluorescence-Lifetime Imaging Microscopy . . . 22
5.4 Lugol staining . . . 23
5.4.1 Lugol's solution ideal concentration test . . . 23

6 Results **24**
6.1 Pigments extraction . . . 24
6.2 Lugol staining . . . 25
6.3 Fluorescence lifetime measurements . . . 27
6.3.1 Time-resolved fluorescence spectroscopy . . . 27
6.3.2 Fluorescence-Lifetime Imaging Microscopy . . . 31

7 Discussion **45**
7.1 *Trichodesmium* IMS101 . . . 45
7.1.1 Lugol staining . . . 45
7.1.2 Time-resolved fluorescence spectroscopy . . . 45
7.1.3 Fluorescence-Lifetime Imaging Microscopy . . . 48
7.2 *Trichodesmium* NIBB1067 . . . 51
7.2.1 Lugol staining . . . 51
7.2.2 Fluorescence-Lifetime Imaging Microscopy . . . 51
7.3 Comparison between IMS101 & NIBB1067 . . . 51

Conclusion **54**

Bibliography **56**

List of Abbreviations **63**

A Attachments **64**
A.1 Comparison between fluorescence and Lugol staining patterns 64

Introduction

Trichodesmium, a filamentous marine cyanobacterium, is a globally prominent nitrogen gas (N_2) fixer, as it is one of the major contributors to oceanic N_2 fixation (Capone et al. (1997)). Although nitrogenase, the enzyme that catalyses N_2 fixation is irreversibly inactivated by molecular oxygen, *Trichodesmium* is able to conduct both oxygen-evolving photosynthesis and N_2 fixation during the daytime (Capone et al. (1997)). Most (all, except *Oscillatoriales*, to which belongs also *Trichodesmium*) filamentous cyanobacteria for this purpose evolved specialised, differentiated, non-photosynthetic cells called heterocysts. However, these were not found in *Trichodesmium*. Several potential explanations for this long-standing paradox have been suggested, but no definitive answer has been established yet.

Moreover, contrasting findings on nitrogenase regulation have been obtained on two strains of the species *Trichodesmium erythraeum* (IMS101 and NIBB1067). For IMS101, studies using immunoassays reported specialised cells, termed diazocytes, where nitrogenase would be compartmentalised (Bergman and Carpenter (1991)). However, in NIBB1067 no cells with a similar appearance to diazocytes were found (Ohki (2008)).

More recently, a hypothesis involving reversible uncoupling and coupling of phycobiliproteins from and to photosystems has been introduced (Kupper et al. (2004), Küpper et al. (2009)). This hypothesis associates N_2 fixation with cells with high basic fluorescence yield (F_0) resulting from reversible uncoupling of the phycobilisome (PBS) antennae from the photosystem II (PSII) reaction centre and surplus of free PBS (Kupper et al. (2004)).

Uncoupling of PBS from photosystem II (associated with N_2 fixation), proposed by this hypothesis, will prevent energy transfer from PBS to Chl-a. In the absence of other quenching mechanisms, this will necessarily lead to a significant increase in the observed fluorescence lifetime of PBS due to the fact that the free phycobiliproteins exhibit fluorescence lifetime in the order of 10^{-9} s while in the coupled PBS it is by about an order of magnitude shorter (Grabowski and Gantt (1978), Acuña et al. (2018)).

In this master thesis, photophysiological characteristics related to the hypothesis introduced by Kupper et al. (2004) were compared between the *Trichodesmium* IMS101 and NIBB1067 strains. First, the bulk pigment composition of both strains was compared, prior to single cell level analyses.

Second, in order to confirm our assumption of the fluorescence lifetime extension, fluorescence lifetime measurements were performed on a bulk level (Time-resolved fluorescence spectroscopy) to see whether the fluorescence lifetime (τ) differs between *Trichodesmium* filaments that are grown under diazotrophic and non-diazotrophic conditions, respectively. Afterwards, τ was analysed at single-cell resolution to see its spatial distribution within the filaments, using Fluorescence-lifetime imaging microscopy (FLIM). Lastly, simultaneous visualisation of diazocytes (using Lugol's solution, a commonly used marker of N_2-fixing cells (Sandh et al. (2009))) and fluorescence lifetime patterns allowed us to directly relate fluorescence lifetime to N_2 fixation.

1. Photosynthesis

Photosynthesis is a unique biological process of light energy conversion into chemical energy (Nelson and Yocum (2006)). Some of the created chemical energy is stored in carbohydrates (in general CH_2O), which are synthesised from carbon dioxide (CO_2) and an electron donor (H_2A). The general equation for photosynthesis, proposed by Van Niel et al. (1942) is:

$$CO_2 + 2H_2A \xrightarrow{\text{light}} (CH_2O) + 2A + H_2O \tag{1.1}$$

Photosynthetic organisms, called phototrophs, include higher plants, algae (diatoms, phytoplankton, green algae) and bacteria (cyanobacteria and anoxygenic photosynthetic bacteria). The first organisms known to have produced oxygen via photosynthesis are cyanobacteria, which therefore played a key role in the oxygenation of the atmosphere ∼2.3 Ga ago (Holland (1997)). Cyanobacteria, are prokaryotic organisms. Unlike eukaryotic plants and algae, they do not have membrane-bound nucleus, chloroplast, mitochondria and other organelles. Instead, they have double outer cell membrane and folded inner thylakoid membranes, where both photosynthesis and respiration occurs.

1.1 Marine carbon cycle

Carbon (C) is a vital chemical element present in all living things, rocks and sediments, in the atmosphere and ocean. The circulation of C around the Earth is called *carbon cycle*. The ocean plays a dominant role in the carbon cycle. The total amount of carbon in the ocean represents ∼95% of all the carbon at the Earth's surface. Although the amount of carbon stored in marine organisms is small compared to land organisms (∼3 Gt C and ∼610 Gt C, respectively (Schlesinger and Bernhardt (2013))), they fix approximately 50 Gt of inorganic carbon annually, almost half of the total global primary production (Kwiatkowski et al. (2018)).

In the ocean, there is a strong vertical gradient in the concentration of dissolved inorganic carbon (DIC)[1], which comprises aqueous CO_2, carbonic acid (H_2CO_3), bicarbonate ions (HCO_3^-), and carbonate ions (CO_3^{2-}) (Volk and Hoffert (1985)). Physical, chemical and biological processes, referred to as *ocean carbon pumps*, are necessary to maintain this vertical gradient.

There are three vertical pumps in the marine carbon cycle that sequester atmospheric carbon in deep-water and sediments. In the (1) solubility pump, CO_2 gets dissolved into the seawater, and when DIC is mixed with dense, cold water at high latitudes it sinks to the deep ocean. In the (2) carbonate pump, the bio-precipitation of calcium carbonate ($CaCO_3$) in the upper waters is accompanied by the release of CO_2 to the atmosphere. In the (3) biological pump, CO_2 is absorbed into the photosynthetic marine organisms, converting the inorganic C into organic matter that becomes part of the pelagic food chain. The organic C is released back into inorganic either by respiration of the organisms or by their death and subsequential decay (organic C forms high density particles that sink) (Legendre et al. (2015)).

[1] In the deep waters below 1200 m, there is 2284 μmol kg^{-1} and in the surface mixed layer, there is 2012 μmol kg^{-1} (Volk and Hoffert (1985)).

1.2 Oxygenic photosynthesis

The process of oxygenic photosynthesis can be expressed as a redox reaction driven by light energy, where the electron donor from the equation 1.1 is water (H_2O) which is oxidised and oxygen (O_2) is released:

$$CO_2 + 2H_2O \xrightarrow{\text{light}} (CH_2O) + O_2 + H_2O \tag{1.2}$$

(Van Niel et al. (1942)). The equation 1.2 is a summary of two stages, the so-called light and dark reactions. During the light reactions, which are bound on thylakoid membrane, the light energy is converted to chemical energy providing a biochemical reductant nicotine adenine dinucleotide phosphate (NADPH) and a high energy compound adenosine triphosphate (ATP). During the dark reactions, which take place in the stroma (in eukaryotic cells) or in carboxysomes (in cyanobacteria), NADPH and ATP formed in the former stage are utilised to reduce CO_2 to carbohydrates (Masojídek et al. (2013)). This assimilation of inorganic carbon into organic compounds is called carbon fixation.

1.2.1 Photosynthetic light reactions

The light reactions are made up of three phases, (1) light absorption and energy delivery by antenna systems, (2) primary electron transfer in reaction centres, and (3) energy stabilisation by secondary processes (Blankenship (2021). Emphasising the basic principles, each of the phases will be now briefly explained.

Firstly, light energy in the form of photon of a specific wavelength is absorbed by one of the photosynthetic pigments (mostly in the light-harvesting antenna), creating an excited state. This electronic excited state migrates from one antenna pigment to another and eventually ends in the reaction centre (RC).

Secondly, when the energy from the antenna system is transferred into a special dimer of pigments in the RC, this excited pigment (P) loses an electron to a nearby electron acceptor molecule (A), creating an ion-pair state P^+A^-. Next, to avoid recombination (transfer of electron from A^- back to P^+), rapid secondary reactions spatially separate the positive and negative charges, by transfer of an electron to a secondary acceptor (Blankenship (2021)).

The energy stabilisation is achieved by a non-cyclic electron transfer chain (Fig. 1.1). The oxygen-evolving photosynthetic organisms have two photochemical reaction centres, known as Photosystem (PS) I and PSII. In PSII, H_2O is oxidised to O_2, which is released as a waste product (Ruben et al. (1941)). The extracted electrons are transported between PSII and PSI via plastoquinones, two-electron carriers, and the cytochrome b_6/f complex. During the electron transfer, protons are transferred across the thylakoid membrane, creating a protonmotive force which is subsequently used by the ATP synthase to create ATP (Blankenship (2021)).

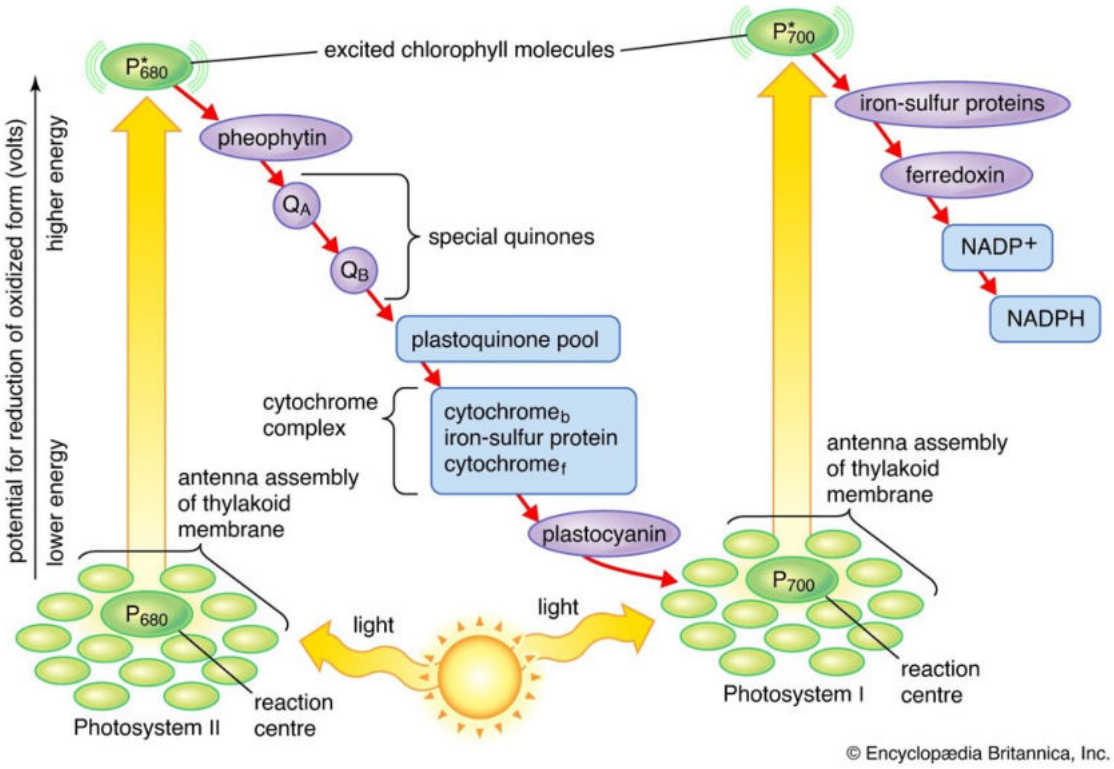

(a)

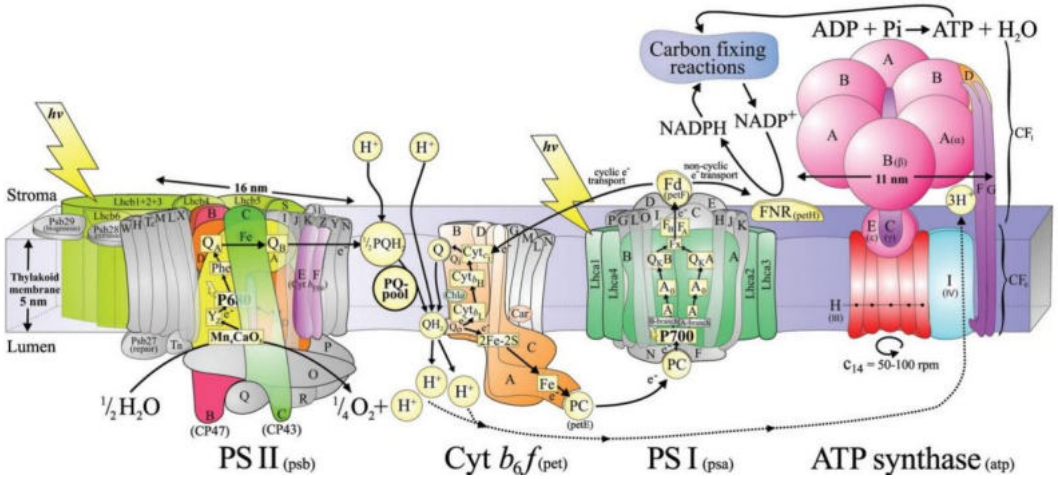

(b)

Figure 1.1: Schematic diagram of the non-cyclic electron transfer chain in oxygenic photosynthetic organisms. The upper diagram (a) is an energetic picture of the flow of electrons, incorporating the major reactions of the light stage into so-called Z-scheme of photosynthesis. The lower diagram (b) is a spatial picture, showing the major protein complexes in the thylakoid membrane whose energetics are shown in the Z-scheme. (a) Source: Encyclopedia Britannica (1998). (b) Source: Blankenship (2021)

Light-harvesting antennae

The light-harvesting complexes, consisting of a number of photosynthetic pigments, are used to increase the cross-section area of the RC in order to collect more of the

incoming light (Blankenship (2021)). The concept of the antenna is shown in Figure 1.2a. Antenna systems often incorporate a funneling mechanism, in which pigments absorbing at the shortest wavelengths (λ) are at the periphery of the complex and the ones absorbing at the longest λ are at the core. In this way, energy is funneled to the RC placed energetically downhill (see Fig. 1.2b) (Masojídek et al. (2013)). Almost all antenna pigments[2] are specifically associated with proteins responsible for their specific functions (Blankenship (2021)).

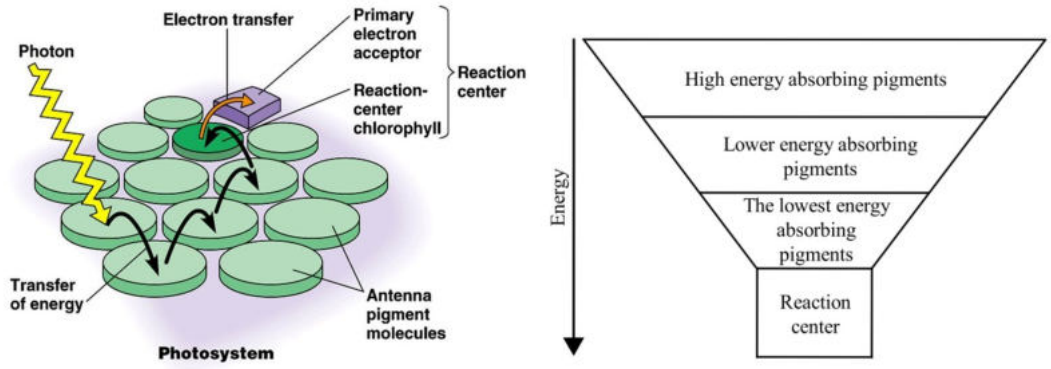

(a) (b)

Figure 1.2: The principle of light-harvesting antennas in photosynthetic organisms. (a) Light is absorbed by a pigment either in the antenna pigments or in the reaction center (RC) chlorophyll. Through the antenna system the energy transfer involves migration of electronic excited states which eventually get to the RC where electron transfer takes place, creating an oxidised electron donor and a reduced electron acceptor. (b) The funnel concept of the antenna complexes. The excitation transfers from the pigments absorbing at shorter wavelengths to the ones absorbing at longer wavelengths. (a) Source: Campbell et al. (1996). (b) Source: Blankenship (2021).

Light-harvesting complexes are present in all chlorophyll-based photosynthetic organisms (Green et al. (2003)). They are found in a wide variety which often define the group of photosynthetic organisms. In this thesis, only the cyanobacterial type, phycobilisome, will be described.

Phycobilisomes (Fig. 1.3 are multimeric extrinsic[3] antenna complexes of PSII in cyanobacteria, red algae and glaucophytes (Sukenik et al. (2009)). Cyanobacterial phycobilisomes have a fan-like arrangement composed of rods connected to a central core which are made up from two or more types of covalently linked tetrapyrrole chromophores attached to proteins known as biliproteins (Shively et al. (2009)). The core is attached to the stromal side of the thylakoid membrane, near to PSII. The most common phycobilisomes are phycoerythrin, phycocyanin and allophycocyanin. They differ in protein identity, chromophore type and relative location in the phycobilisome complex which is given by their absorption spectrum (so the funneling mechanism is met) (Blankenship (2021)).

The phycobilisomes of the cyanobacterium of our interest, *Trichodesmium*, are dominated by the phycobiliprotein phycoerythrin (PE) which has absorbance peaks

[2]The only exception is the chlorosome antennae, containing bacteriochlorophyll, where pigment-pigment interactions are the most important (Cohen-Bazire et al. (1964)).

[3]The antenna is anchored to thylakoid membranes, but does not itself span the membrane (Blankenship (2021)).

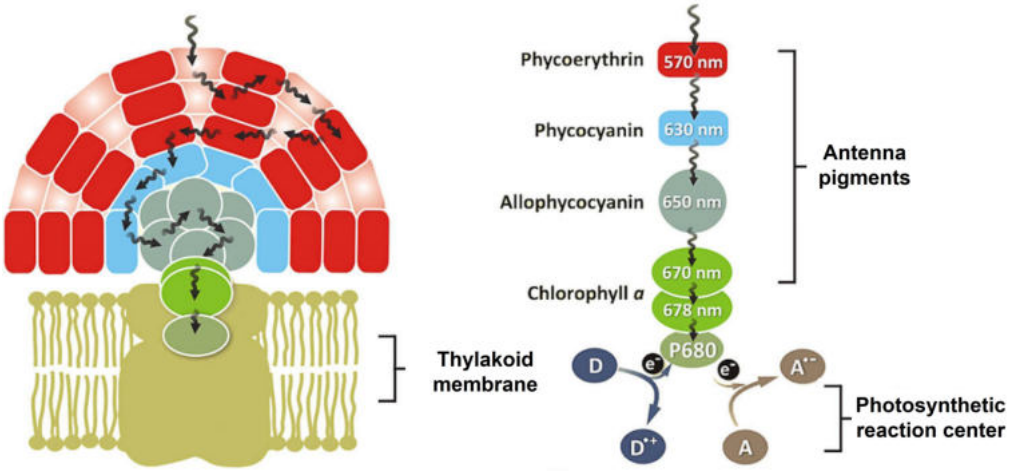

Figure 1.3: Schematic model of a phycobilisome structure located on the thylakoid membrane and the energy transfer steps through the antenna (incorporating the funnel concept) including the charge separation Figure adapted from aquaportail (2020)

at 490–500 nm due to its brown phycourobilin (PUB) component and at 545–565 nm for its red phycoerythrobilin (PEB) component. The phycobilisome also contains the blue-green phycocyanin (PC), which absorbs at 620 nm, and the blue allophycocyanin (AP), which absorbs at 650 nm (Hynes et al. (2012)).

1.2.2 Photosynthetic dark reactions

In the last, not directly light-dependent stage of photosynthesis, the high-energy molecules NADPH and ATP that are not suitable for long-term storage of energy are converted into more stable compounds (mostly sugars) using CO_2. This transformation, referred to as carbon fixation occurs in the so-called Calvin-Benson cycle (1.4).

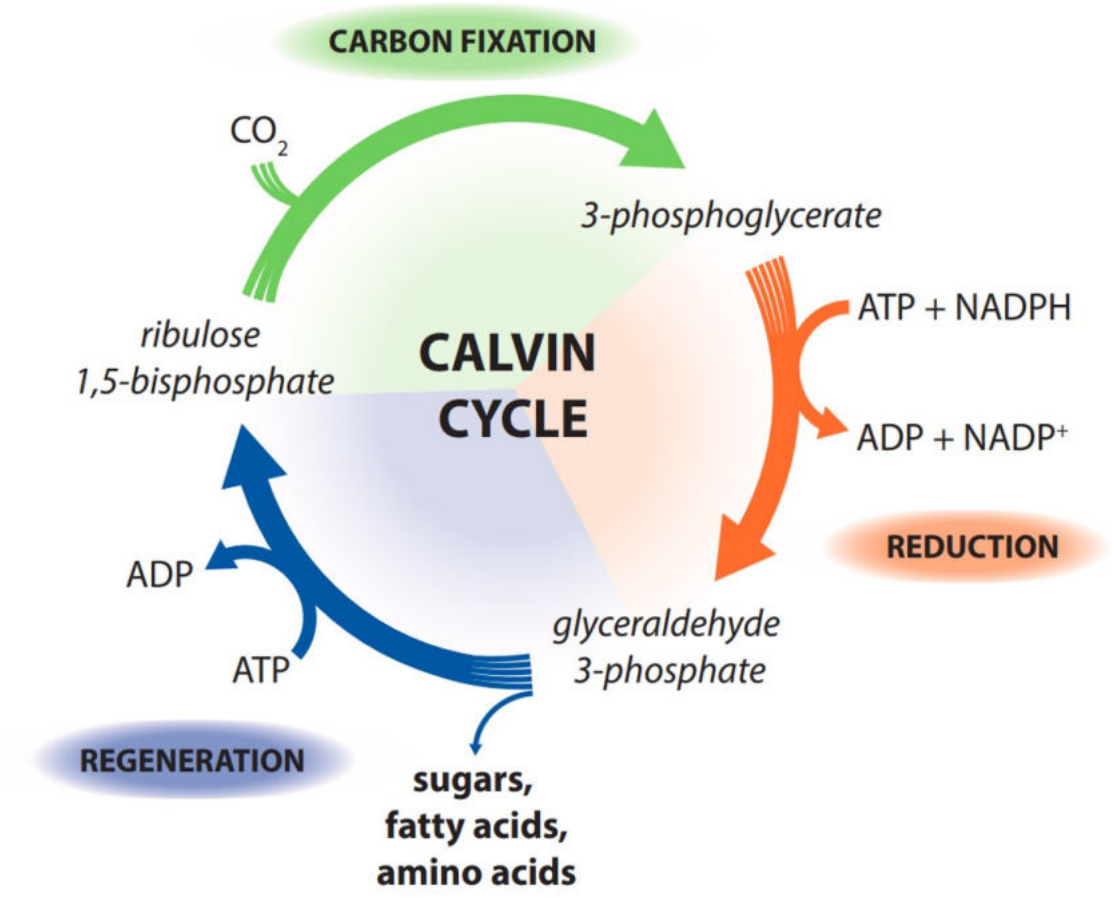

Figure 1.4: Carbon fixation in the dark reactions of photosynthesis with its three stages: fixation, reduction and regeneration. Source: MCB (2007).

2. Nitrogen fixation

Nitrogen (N), as a part of essential organic substances such as proteins or nucleic acids, is an indispensable element crucial for life (Postgate (1998)).

2.1 Marine nitrogen cycle

Nitrogen exists in different forms, which are all interrelated in the nitrogen cycle (Fig. 2.1), one of the most important and complex biogeochemical processes on Earth (Gruber (2008)). Dinitrogen gas (N_2), despite being the largest reservoir of N, as it composes 78% of our atmosphere and can be found dissolved in the ocean, is not biologically available for most organisms, due to its relatively stable triple bond (Zehr and Capone (2021), Karl and Michaels (2001)). To emphasise this, all nitrogen forms except N_2 are referred to as "fixed" (Gruber (2008)). However, there are certain organisms able to convert (fix) N_2 into ammonium (NH_4^+), which can then, in the oceans, be taken up by phytoplankton. The process where nitrogen is incorporated into living organisms is called "assimilation". When organisms die and are decomposed, the assimilated nitrogen is released back to the ocean in form of ammonium in the euphotic zone, and as "particulate organic nitrogen" (PON) and "dissolved organic nitrogen" (DON) which sink below the euphotic zone ("dark ocean", aphotic zone and sediments). PON and DON can be converted back to NH_4^+ through the food web, in a process called remineralisation. In the nitrification process some bacteria and archaea below the euphotic zone can oxidise ammonium, releasing nitrite (NO_2^-), which is then oxidised to nitrate (NO_3^-) by different nitrite-oxidising microbes. Both NO_2^- and NO_3^- can be resupplied to the euphotic zone via upwelling, where they can be assimilated by phytoplankton, continuing with the nitrogen cycle. Dissimilatory nitrate reduction to ammonium (DNRA) is the reduction of nitrate via nitrite to ammonium with organic or inorganic electron donors (Giblin et al. (2013)). While DNRA recycles fixed N in the ecosystem, a similar process called denitrification contributes to its removal (Gao et al. (2012)). In this process, mediated by facultative anaerobic bacteria, nitrate and nitrite are reduced back to nitrogen gas which is released to the atmosphere (De Mandal et al. (2020)). Another process leading to loss of nitrogen from the marine system is anaerobic ammonia oxidation (anammox) in which NH_4^+ is oxidised to molecular N_2 with NO_2^- as the terminal electron acceptor (Rysgaard et al. (2004)).

Nitrate and ammonium are bioavailable N, however, many organisms prefer NH_4^+ since its assimilation requires less energy than the assimilation of NO_3^- (which is mediated through a redox reaction) (Zehr and Ward (2002)).

2.2 N_2 fixation

In order to counterbalance the loss of nitrogen from the marine ecosystem, input of new bioavailable forms of N is crucial. This is provided mainly by N_2 fixation, a globally significant process in which the stable triple covalent bond between two nitrogen atoms is broken to produce ammonia or nitrate (Taiz and Zeiger (2002), Mahaffey et al. (2005)).

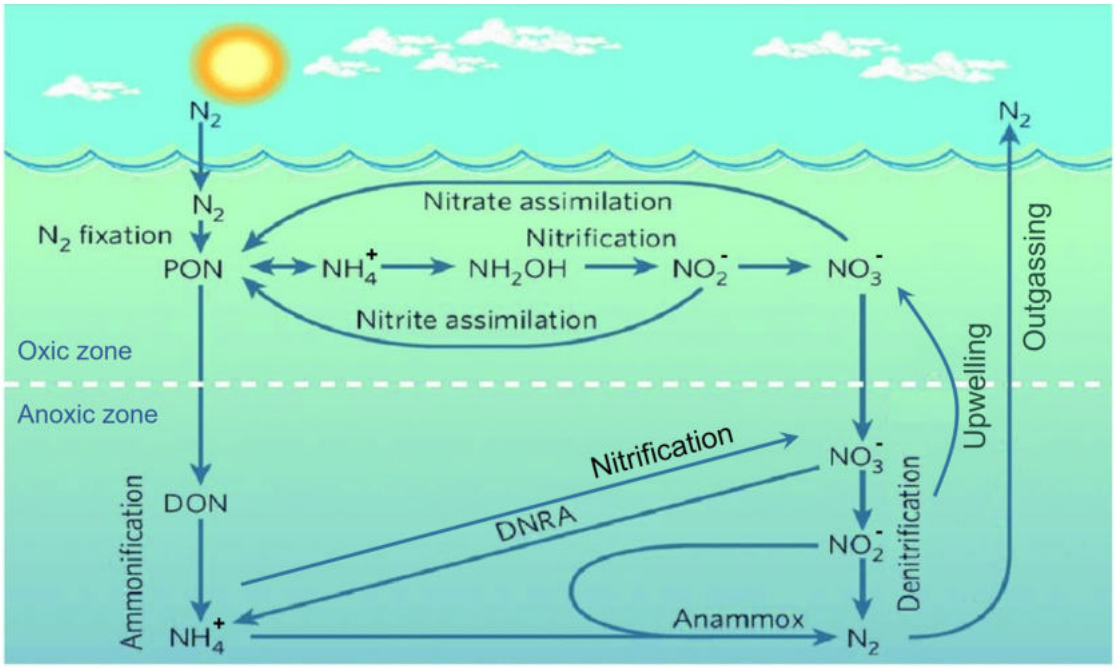

Figure 2.1: Marine nitrogen cycle with gain of nitrogen through nitrogen fixation and loss through anammox and denitrification followed by outgassing. Figure adapted after Arrigo (2005).

One way of natural N_2 fixation happens by lightning, where the energy of lightning ionises the N_2 molecules from the atmosphere, allowing them to form nitrogen oxides, which are dissolved by rain and transported to the ocean. However, only about 10% of the total N_2 yield is fixed through this process. The major source of fixed N_2 derives from the activities of free-living and symbiotic archaea and bacteria, termed diazotrophs. There are no eukaryotes able to fix nitrogen, except when in symbiosis with some bacteria or archaea (Zehr and Capone (2021)). Apart of the naturally occurring N_2-fixation, there are ways of industrial ammonia synthesis (Leigh (2002),Galloway et al. (2008)).

The overall reaction in the biological nitrogen fixation (BNF) process, is following:

$$N_2 + 16ATP + 8H^+ + 8e^- \rightarrow 2NH_3 + H_2 + 16ADP + 16P_i \tag{2.1}$$

(Postgate (1998), Seefeldt et al. (2020)). Ammonia (NH_3) is then protonated, creating ammonium (NH_4^+). As can be seen in equation 2.1, BNF requires a considerable amount of energy and electron donors. Moreover, an equimolar amount of hydrogen (H_2) is formed concurrently, contributing to the high energy costs of BNF (Hoffman et al. (2014)).

BNF is catalysed by nitrogenase, a highly conserved two-component enzyme complex (Postgate (1998)). The two structural proteins that compose it are dinitrogenase (component I) and dinitrogenase reductase (component II) (Bulen and LeComte (1966)). The most common dinitrogenase and dinitrogenase reductase are encoded by *nifHDK* genes, and the expressed proteins are the heterotetrameric MoFe and homodimeric Fe protein (Dixon and Kahn (2004)). The former, encoded by *nifDK*, catalyses the reduction of N_2 to NH_3, whereas the latter, encoded by *nifH*, binds ATP and transfers electrons from ferredoxin to dinitrogenase (Leigh (2002)).

The expression of both protein subunits is necessary for nitrogenase activity.

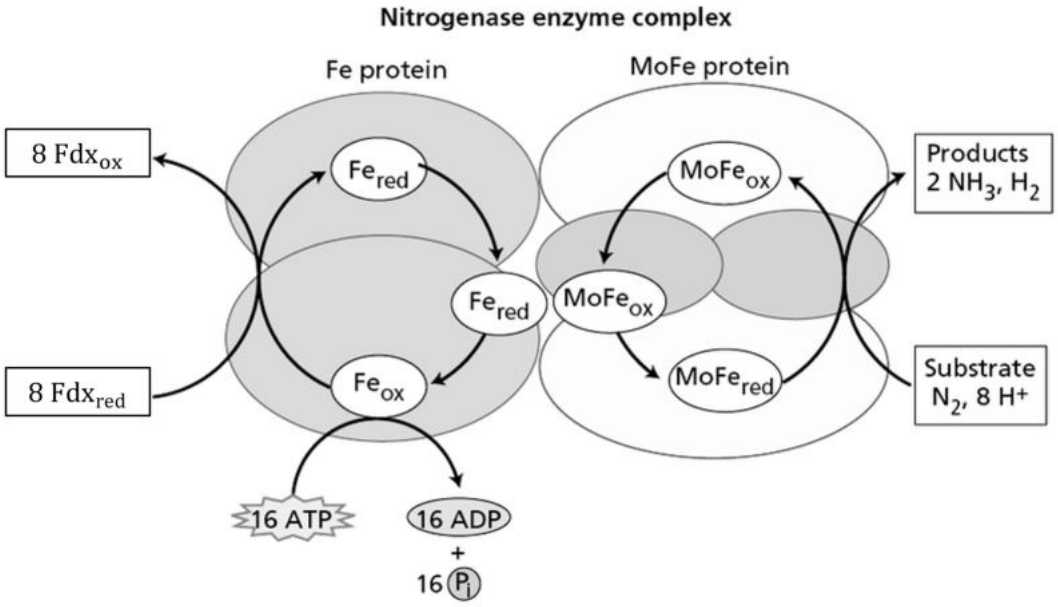

Figure 2.2: The enzymatic complex of nitrogenase catalysing the BNF reaction. Fe protein is reduced by Ferredoxin. Binding and hydrolysis of ATP to the Fe protein causing a confomational change on the Fe protein facilitating the redox reactions. The Fe protein reduces the MoFe protein which subsequently reduces N_2. Figure adapted after Taiz and Zeiger (2002).

There are three hypotheses about when and how N_2 fixation first evolved. The "archaea-first hypothesis" claims that it evolved in archaea and was later transferred to bacteria (Raymond et al. (2004), Hamilton et al. (2011), Koirala and Brözel (2021)). An alternative hypothesis states that the evolution of nitrogen fixation happened in the last universal common ancestor (LUCA) (Weiss et al. (2016), Raymond et al. (2004)). The third, the "bacteria-first hypothesis", postulates that it first evolved in bacteria, completely opposing the "archaea-first hypothesis". Due to the mutual exclusiveness of these hypotheses, only one can be true (Pi et al. (2022)).

Whichever of the three hypotheses is correct, N_2 fixation took place on Earth already before the oxygenation of the atmosphere by photosynthesising cyanobacteria which happened between 2.4 and 2.2 Ga (Holland (1997)). The change from an anoxic to an oxygenic atmosphere created a huge challenge for diazotrophs since nitrogenase is irreversibly inhibited by molecular oxygen (O_2) via oxidative damage to iron sulphur clusters (Burgess and Lowe (1996)), proteolytic degradation of dinitrogenase reductase (Durner et al. (1996)), and suppression of nitrogenase synthesis and posttranslational modification (Gallon (1992)). The Fe protein (dinitrogenase reductase) is inhibited within seconds whereas the MoFe protein (dinitrogenase) within minutes of oxygen exposure (Gallon (1992)). Hence, diazotrophs had to develop mechanisms to protect their nitrogenase from deleterious O_2 (Berman-Frank et al. (2003)).

The most common protective mechanisms used by oxygen-evolving cyanobacteria capable to fix N_2 under aerobic conditions include either a temporal or spacial

separation of the N_2 fixation and photosynthesis processes. Organisms that follow the time separation usually fix nitrogen at night and photosynthesis is carried out during the day (Fig. 2.3A). These organisms are single-celled cyanobacteria and nitrogenase is typically found in all cells. The spatial separation (Fig. 2.3B) is exhibited mainly by filamentous cyanobacteria which for this purpose produce specialised, differentiated, non-photosynthetic cells called heterocysts (Haselkorn (1978), Janaki and Wolk (1982)). When vegetative cells of heterocystous cyanobacteria are deprived of NH_4^+, 5-10% of the cells undergo differentiation and form thick-walled heterocysts (Gallon (1992)). These cells lack PS II, which makes it impossible to produce oxygen and allows daytime N_2 fixation (Taiz and Zeiger (2002)).

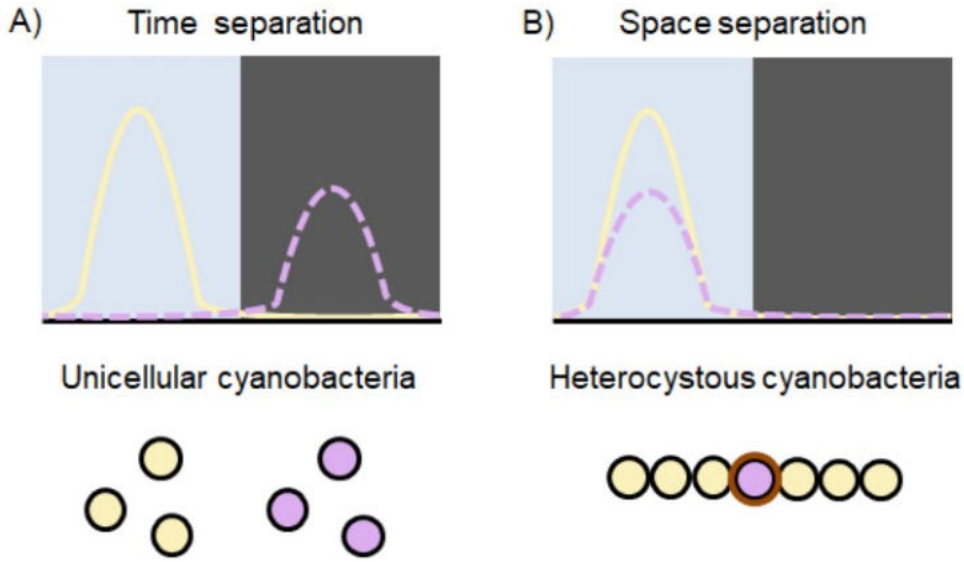

Figure 2.3: Two common protective mechanisms of diazotrophs to protect nitrogenase from oxygen. Pink colour indicates N_2 fixation and yellow indicates photosynthesis. A) Single-celled cyanobacteria fix N_2 during the night, while photosynthesis is carried during the day. B) Filamentous cyanobacteria with fully differentiated N_2 fixing cells, heterocysts, are able to fix N_2 and photosynthesise simultaneously. Figure from Hania et. al., in prep.

The filamentous cyanobacterium *Trichodesmium* is particularly interesting because it fixes N_2 only in the light despite not having heterocysts. *Trichodesmium* is one of few known non-heterocystous species evolving O_2 simultaneously with N_2 fixation. Several O_2-protective mechanisms have been suggested: formation of anoxic microzones within colonies (Paerl and Bebout (1988)) or downregulation of photosynthesis during the peak of N_2 fixation (Berman-Frank et al. (2001b)). Other studies suggest nitrogenase being compartmentalised in a subset of cells (10-20% of total cells) termed as diazocytes (Bergman and Carpenter (1991), Berman-Frank et al. (2001b)). These cells are morphologically different by their reduced number of storage compounds and gas vacuoles (Fredriksson and Bergman (1997)). Moreover, they do not lack PSII and thus are able to photosynthesise (Bergman and Carpenter (1991), Fredriksson and Bergman (1995), Berman-Frank et al. (2001b)). Separation in time is therefore not sufficient and a further complex interaction between both spatial and temporal segregation of photosynthesis, respiratory and N_2 fixation is needed (Berman-Frank et al. (2001b), Chen et al. (1999)).

In this thesis the hypothesis of dynamic reversible uncoupling of phycobilisomes from the photosystems in order to switch between different photosynthetic activity states (Kupper et al. (2004), Küpper et al. (2009)) is re-evaluated using fluorescence lifetime techniques.

3. Trichodesmium

Trichodesmium, a marine filamentous cyanobacterium lives in tropical and subtropical oceans and is found both as single filaments, called trichomes, and colonies (in a puff or tuft shape) consisting of tens to hundreds of filaments which are buoyant due to gas vacuoles (Capone et al. (1997), Hynes et al. (2012)). Each trichome consists of tens to hundreds of cells and each cell is generally 5 to 15 μm in diameter and 4 to 6 μm in length (Hynes et al. (2012), Prufert-Bebout et al. (1993)). The brown or red blooms formed by *Trichodesmium* gave the Red Sea its name (Ehrenberg (1830)).

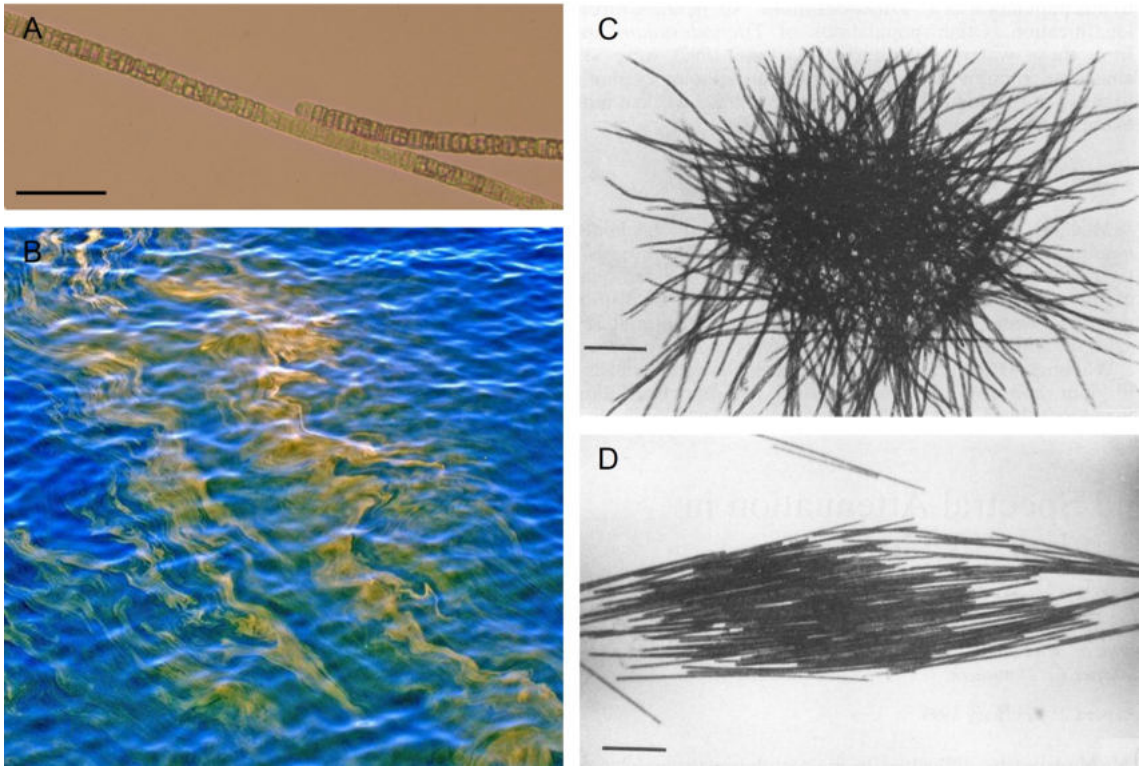

Figure 3.1: Different morphologies of *Trichodesmium*. (A) A single trichome (stained by 2.5% v/v acidic iodine-potassium Lugol's solution). Scale bar, 50 μm. (B) *Trichodesmium* bloom visible on the sea surface. (C) Spherical (puff) cultivated *Trichodesmium* aggregate. (D) Fusiform (tuft) aggregate. Scale bars in (C) and (D), 100 μm. (B) Source: Kolter (2022). (C) and (D) Source: Prufert-Bebout et al. (1993).

Trichodesmium is a non-heterocystous diazotroph providing a significant proportion of nitrogen in oceanic oligotrophic systems (Capone et al. (1997), Mahaffey et al. (2005)). Due to this global importance, *Trichodesmium* has long been the focus of many studies dealing primarily with the mechanisms behind the simultaneous occurrence of the mutually exclusive processes of nitrogen fixation and photosynthesis. Although several potential explanations have been proposed, no definitive answer has yet emerged.

Six species of *Trichodesmium* are documented in the literature. In this thesis our subject of study is the species *Trichodesmium erythraeum* (hereinafter only *Trichodesmium*), first described by Ehrenberg (1830). Specifically, all the mea-

surements were done on the closely aligned strains IMS101, isolated from North Atlantic coastal waters by Hans Paerl's group (Prufert-Bebout et al. (1993)), and NIBB1067, isolated from Kuroshio waters by Ohki Kaori (Ohki and Fujita (1982)). Although being the same species, contradictory results have been shown about these two strains. While in IMS101 nitrogenase is present only in a subset of cells along filaments (Berman-Frank et al. (2001b)), in NIBB1067 it is found almost in all cells (Ohki (2008)). Since most of the previous research about *Trichodesmium* has been conducted on one of these two strains, this strain-specific differences could be one of the reasons why this N_2 fixation-related enigma has not been solved yet.

3.1 Reversible uncoupling of phycobiliproteins

In the studies of Berman-Frank et al. (2001b), using the Chl fluorescence kinetic microscopy (FKM; Küpper et al. (2000)), it was shown that *Trichodesmium* cells have a homogeneous high photosynthetic yield during the non-N_2-fixing hours (early and late stages of the light phase). During the period of N_2 fixation (5 to 7 hours after the beginning of the light phase) some cells (termed "bright cells"), evenly distributed along trichomes, showed about two times higher dark-adapted fluorescence yield (F_0) compared to other cells. Additionally, cells could switch between fluorescence states within 10 to 15 min. This indicates the possibility for all the cells being photosynthetically active during the light phase and furthermore, that N_2 fixation in *Trichodesmium* is both spatially and temporally separated (Berman-Frank et al. (2001b)).

In the subsequent studies (Kupper et al. (2004)), four activity states were observed: (I)"bright cells", (II)"very bright cells", (III) cells with a low-fluorescent state and (IV) a normal non-N_2-fixing state. Reversible transitions between all four states were observed to happen in range of minutes, sometimes even seconds, which excluded involvement of pigment synthesis/degradation. Instead, reversible (un)coupling of the phycobilisome antenna from PSII reaction centres was suggested as the mechanism behind the fast changes in fluorescence intensity.

The type I, "bright cells", appearing only in the middle of the light phase, were assigned to as N_2 fixing. The fluorescence characteristics of these cells (measured as variable fluorescence, $F_v = F_m - F_0$) indicated active PSII, which implied a necessity for involving a mechanism such as the Mehler reaction that would up-regulate the O_2-scavenging processes (Kupper et al. (2004)). During this activity state, state II to state I transition (uncoupling of the phycobilisome antenna from PSI and coupling to PSII) might be occurring resulting in a surplus of free phycobilisomes due to the high PSI:PSII ratio characteristic for *Trichodesmium* (Berman-Frank et al. (2001a)). This excess of uncoupled PBS are most probably behind the two- to threefold higher F_0 of the bright cells (Kupper et al. (2004)).

The type II, "very bright cells", appearing independently on the N_2-fixing hours had F_0 more than three times higher than the normal F_0 and low variable fluorescence F_v suggesting hardly any PSII activity (Kupper et al. (2004), Küpper et al. (2009)) and thus a complete uncoupling of the PBS antenna from both photosystems. These cells are most probably related to stress (Kupper et al. (2004)).

Cells with a low-fluorescence state and diminished photochemical activity were observed mainly after the type I state. These cells may represent a fluorescence-quenching recovery period after which they become normal, non-diazotrophic cells

(Kupper et al. (2004)).

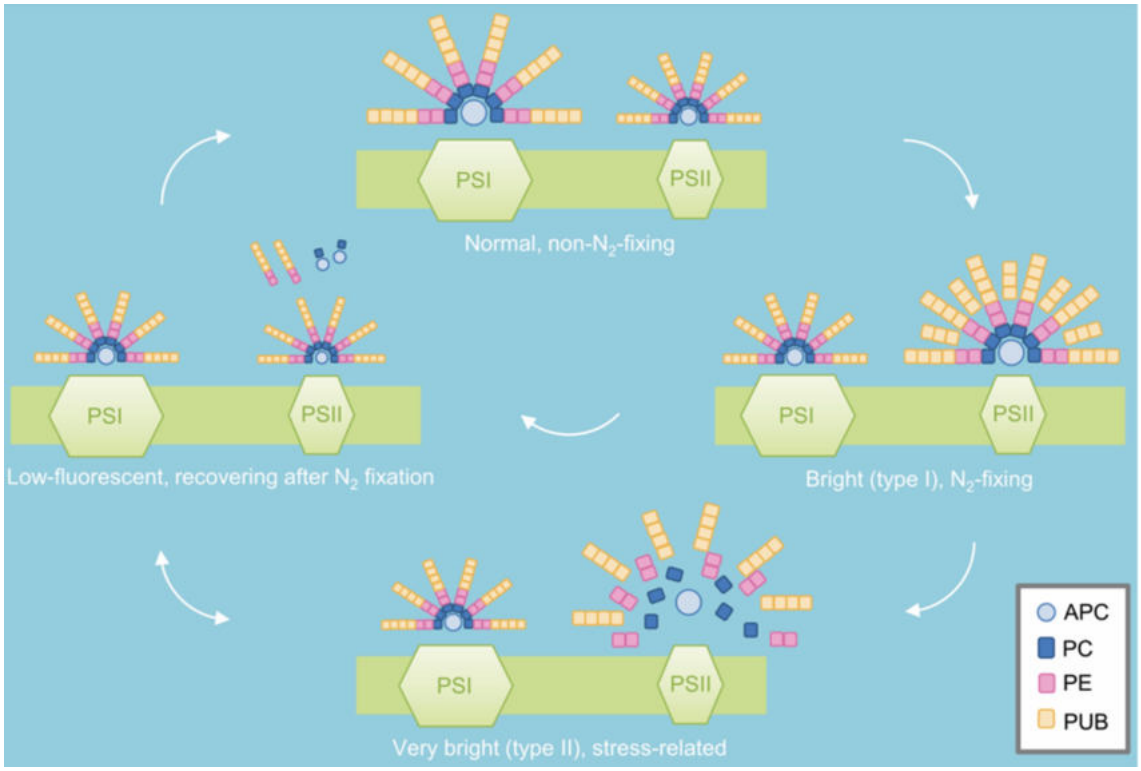

Figure 3.2: Model of the reversible phycobiliprotein uncoupling from the photosystems related to nitrogen fixation proposed by Küpper et al. (2009). The bigger size of PSI compared to PSII is representative of the high PSI:PSII ratio in *Trichodesmium*. APC - allophycocyanin; PC - phycocyanin; PE - phycoerythrin. Figure from Hania et. al., in prep.

4. Fluorescence

Deexcitation of electronically excited state that give rise to emission of radiation is called radiative transition. If the emitted radiation is generated in the course of transitions between states of the same multiplicity, it is called fluorescence. The energy of the emitted radiation is lower than that used to create the excited state (Gilbert and Baggott (1991), Atkins and Friedman (2011)). The Figure 4.1 illustrates all the possible transitions that may occur between the different energy levels.

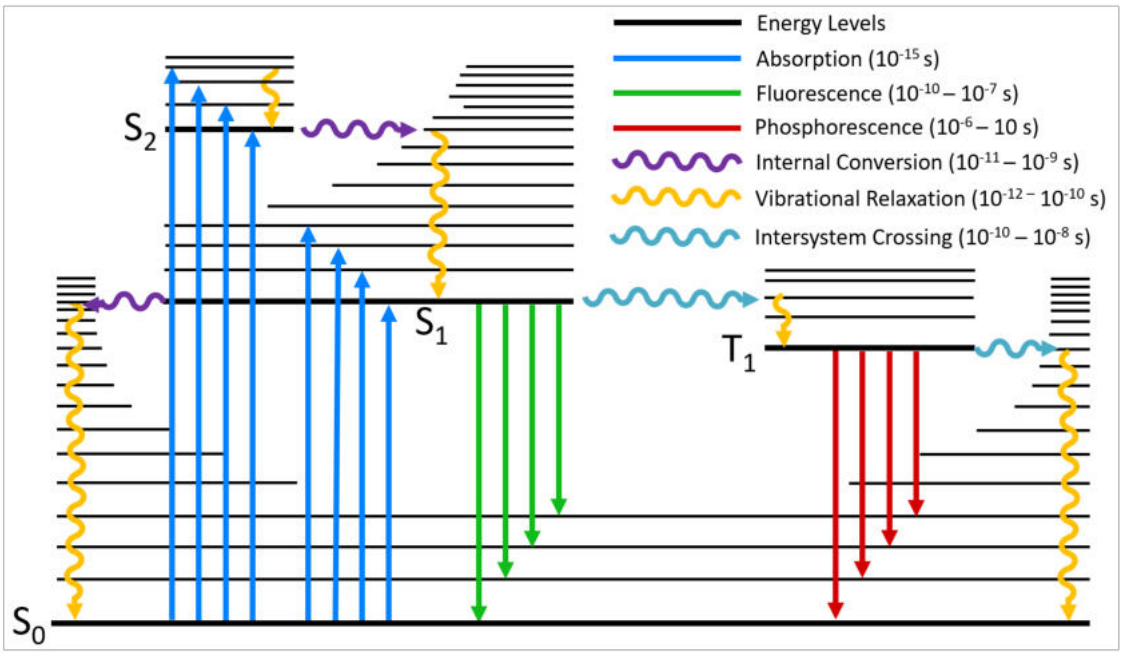

Figure 4.1: A typical Jablonski diagram showing the possible radiative and non-radiative transitions. Absorption of a photon with specific energy excites a molecule from its ground electronic state level S_0 to either a singlet first S_1 or second S_2 electronic excited state. At each energy level, fluorophores can exist in a number of vibrational energy levels (represented by the multiple lines in each electronic state) from which they relax to the lowest one, releasing the energy as heat. From this state, transition to to one of the vibrational levels of S_0 occurs by emitting a photon. From the S_1 level, intersystem crossing to the triplet state T_1, involving change of electron spin multiplicity, can occur. Phosphorescence, a very slow radiative transition, is one possible route back to S_0 (Lakowicz (1999)). Figure from Edinburch Instruments (2022).

4.1 Fluorescence lifetime and its measuring

A characteristic feature of fluorescence is its lifetime. The fluorescence lifetime is the average time that a molecule remains in its excited state before returning to the ground state. Since the return of the excited electron to the ground state is spin-allowed, it occurs rapidly and the fluorescence lifetimes of isolated organic fluorophores are typically in the range 10^{-9}-10^{-11} s (Lakowicz (1999)).

For an ensemble of molecules excited by the absorption of a photon, the excited state population $n(t)$ will evolve as

$$dn(t)/dt = -kn(t) \tag{4.1}$$

(Gilbert and Baggott (1991), Jain et al. (2009)), hence, the number of excited molecules decays exponentially:

$$n(t) = n_0 e^{-kt} \tag{4.2}$$

where n_0 denotes the initially ($t = 0$) excited population. The value of the rate constant k (its reciprocal value is the time constant, τ) is determined by probabilities (rates) of all the possible deexcitation pathways (Gilbert and Baggott (1991)). These are the nonradiative processes, that include internal conversion, intersystem crossing, energy transfer and photochemical reactions, and the radiative process fluorescence. Thus:

$$k = 1/\tau = k_r + k_{nr} \tag{4.3}$$

(Gilbert and Baggott (1991)), where the nonradiative processes are grouped under a single rate constant, k_{nr}. In a time-resolved fluorescence experiment, only the photons emitted by the decaying excited molecules are detected, hence the expression for the fluorescence decay includes the radiative rate constant:

$$y(t) = k_r n_0 e^{-kt} \tag{4.4}$$

The total number of photons emitted is obtained by integrating eq. 4.4 over time:

$$n_{em} = \int_0^\infty y(t)\, dt = \int_0^\infty k_r n_0 e^{-kt}\, dt = n_0 \frac{k_r}{k_r + k_{nr}} \tag{4.5}$$

where in the fraction on the right side of the equation we recognise the definition of the fluorescence quantum yield, $\Phi = k_r/(k_r + k_{nr}) = n_{em}/n_0$ (Gilbert and Baggott (1991), Jain et al. (2009)).

We see that the kinetics of fluorescence track the kinetics of the excited state. In practice, in a time-resolved fluorescence measurement, the signal emitted from the sample is detected only from a certain direction, not from all the photons emitted from the sample. Moreover, all the photons emitted from an ensemble of molecules will not have the same energy, instead, their energies will be distributed according to the molecule's emission spectrum. Thus, the actual measured fluorescence signal will also depend on the wavelength at which it is detected. The time-dependent photon count $f(t)$ will be:

$$f(\lambda, t) = f_0(\lambda) e^{-kt} \tag{4.6}$$

where the wavelength-dependent initial amplitude $f_0(\lambda)$ has the shape of the steady-state emission spectrum of the molecule. The rate constant is independent of the measurement wavelength. In a typical fluorescence experiment, the sample is subjected to a short pulse of light and then the number of photons arriving at the detector during a given time interval after the pulse $t + dt$ is counted. This is the basis of the time-resolved fluorescence method called *time-correlated single photon counting* (see 4.1.1). The output of such measurement is a *histogram* of the photon arrival times.

This offers an intuitive way to understand the physical meaning of the time constant $\tau = 1/(k_r + k_{nr})$. The area-normalised fluorescence decay curve gives the probability distribution of the photon emission, hence we can define the average lifetime of the excited state, $< \tau >$, as:

$$< \tau >= \frac{\int_0^\infty t f(t)\, dt}{\int_0^\infty f(t)\, dt} = \frac{f_0 \tau^2}{f_0 \tau} = \tau \tag{4.7}$$

which just equals the time constant.

If a sample consists of two (or more) species that do not interact between themselves, their decays will be independent and the fluorescence decay at any wavelength where their spectra overlap will be a sum of exponentials:

$$f(\lambda, t) = f_{1,0}(\lambda) e^{-k_1 t} + f_{2,0}(\lambda) e^{-k_2 t} \tag{4.8}$$

(Loefroth (1986)). The wavelength-dependent initial amplitudes $f_{1,0}(\lambda)$ and $f_{2,0}(\lambda)$ form *Decay Associated Spectra* (DAS).

The concept of the average lifetime given in eq. 4.7 can be straightforwardly extended to multiexponential decays, for two components (Li et al. (2020)):

$$< \tau >= \frac{f_{1,0}(\lambda)\tau_1^2 + f_{2,0}(\lambda)\tau_2^2}{f_{1,0}(\lambda)\tau_1 + f_{2,0}(\lambda)\tau_2}. \tag{4.9}$$

The average lifetime computed in eq. 4.9 is denoted *intensity-weighted lifetime* τ_I. It should be kept in mind that in a mixture, this is in general a wavelength-dependent quantity.

The fluorescent pigments in photosynthetic samples are typically bound to proteins in order to form well organized arrays in which energy transfer occurs, thus they do not act independently. The excited-state dynamics of such system can be described by a coupled set of linear differential equations; for two species:

$$\begin{aligned} dn_1/dt &= -(k_{11} + k_{12})n_1 + k_{21} n_2 \\ dn_2/dt &= k_{12} n_1 - (k_{22} + k_{21}) n_2 \end{aligned} \tag{4.10}$$

where n denotes the number (concentration) of molecules in the excited state, we dropped the explicit time-dependence from the expressions for clarity. The above system of equations can be expressed in a compact vector form:

$$d\mathbf{n}/dt = K\mathbf{n} \tag{4.11}$$

where the off-diagonal elements of matrix K represent the pairwise rate constants for energy transfer between the species. The elements k_{11} and k_{22} are the rate constants of the excited state decays of molecules when isolated. In a general case, where the excitation energy betwen species occurs, the experimentally observed kinetics will still be a sum of exponentials as in eq. 4.8, but with the rate constants now corresponding to the eigenvalues of the matrix K. The special case of a mixture of independently decaying species is in the present formalism described by K that is diagonal, elements k_{12} and k_{21} are set to 0 and the DAS corresponding to the experimentally observed rates (i.e. k_{11} and k_{22}) represent the emission spectra of molecules.

In a general case, DAS assigned to the observed decay rates no longer have the shapes of the pure emission spectra of the individual species, nevertheless, they can be used to extract valuable information about the system.

An illustration of both time-resolved and spectral fluorescence data and their analysis is shown in Figure 4.2.

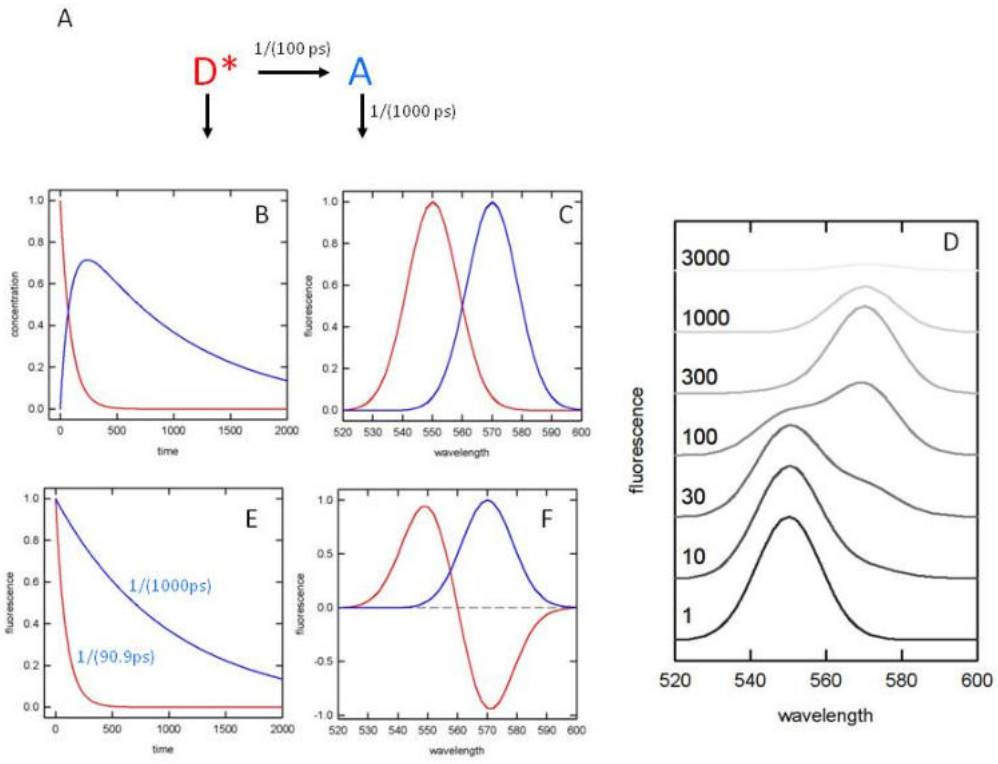

Figure 4.2: A simple kinetics scheme of a process involving a donor (D) and acceptor molecules that both decay with a rate constant of $1/(1000\,\mathrm{ps})$. Also, there is energy transfer from donor to acceptor. In addition, we assume that both molecules emit fluorescence with the same radiative rate. The systems evolve in time as shown in panel B, emission spectra of the donor and acceptor are given in C. Panel D shows simulated emission spectra of the sample at selected times. It can be seen how initially the fluorescence is mainly detected from the donor and the maximum of emission shifts to the acceptor at later times. The panel E shows the single exponential kinetics that would be obtained by fitting the data by a sum of two exponentials (they give the experimentally observable rates). The corresponding decay-associated spectra (DAS) are given in panel F. The negative peak in the DAS indicates energy transfer.

4.1.1 Time-Correlated Single Photon Counting

Time-Correlated Single Photon Counting (TCSPC) is a conceptually straightforward method for measuring fluorescence decays. At time $t = 0$, the sample is excited by a short light pulse and the arrival time of the emitted photon into the detector is measured. Multiple repetitions of the excitation pulse produce a histogram of photon counts versus time, which correspond to the fluorescence decay kinetics

of the studied sample (O'Connor (2012)). This can be fitted with an appropriate mathematical expression, in this case an exponential function, to yield the lifetime of the excited state. Such measurement can be performed with detection set at different wavelengths, provided the instrument is equipped with a monochromator or a set of band-pass filters. These decays can be processed in parallel, yielding not only the rate constant but also the wavelength-dependent amplitudes of the exponentials that together form the decay-associated spectrum of the sample (DAS, see eq. 4.8).

In reality, the excitation pulse is not a delta function, the detector has a finite time response and there are parasitic signals (e.g. afterpulses) that degrade the signal quality. Both the source and detector features combine to produce the instrument response function (IRF) of the instrument. The signal recorded with a real instrument thus represents the sample fluorescence decay convoluted with the IRF, which has to be recorded separately and included in the analysis. The fitting is then performed by so called iterative re-convolution, in which the fitting function is convoluted with the empirically acquired IRF and the measured decay is then fitted with the resulting curve:

$$I(t) = \int_{-\infty}^{t} IRF(t') \sum_{i=1}^{n} A_i e^{-\frac{t-t'}{\tau_i}} dt' \tag{4.12}$$

(O'Connor (2012)), where $I(t)$ denotes the fluorescence intensity from the sample at time t, originating as a response to an excitation pulse at time t'. A_i is the amplitude of the exponential number i corresponding to the lifetime τ_i.

It should be noted that the utility of the fitting approach to data analysis is limited by the number of photons recorded.

5. Materials and methods

5.1 Culture conditions

Batch cultures of *Trichodesmium erythreum* IMS101 and NIBB1067 were grown at 26 ° C and 200 μmol photons $\cdot\, m^{-2} \cdot s^{-1}$, under white light with a 12:12 h light: dark cycle in 0.2-μm-filtered artificial seawater (YBCII medium; Chen et al. (1996)). Cultures maintained in cell tissue culture flasks were placed on a back-forth plate shaker with 100 rpm continuous agitation and were kept in exponential growth phase by regular replenishment of culture medium.

As a control to the N_2 fixing *Trichodesmium*, half of the cultures were grown in NO_3^--containing media, which inhibits N_2 fixation (Ohki et al. (1991)). $NaNO_3^-$ was added regularly to achieve mean concentrations of 100 μM. Acclimatisation to NO_3^- was done for at least one week before measurements. Concentrations were monitored by UV absorption spectrometry according to Collos et al. (1999).

5.2 Phycobiliprotein extraction

Phycobiliprotein extracts from *Trichodesmium erythraeum* were prepared as described in Rippka et al. (1974). After filtrating on Whatman Cyclopore polycarbonate circles, 5.0 μm, 25 mm, the cultures were frozen in liquid nitrogen. Five mililiter of phosphate buffered saline without potassium salt[1] (prepared as described in Protocols (2007)) were added to each sample. From this step, the samples were continuously kept at 4 °C and all work with the cells was done with minimal light. Using a vortex shaker, the cells were separated from the filter. The filter was removed and cells were lysed for 3×1 min using a sonicator Kraintek 6. The extracts were centrifuged in Eppendorf 5804R centrifuge for 45 min at 4200 rpm at 4 °C. The supernatant was pipetted into a 2 ml eppendorf tube and centrifuged for 15 min at 4200 rpm at 4 °C. 750 μl of the supernatant was pipetted into a quartz microcuvette and absorption spectra from 400 to 700 nm was measured using a UV500, ThermoSpectronic UV/Vis spectrometer. Blank spectra of the medium YBCII with the phosphate buffer were substracted from the absorption spectra of the samples. Replicate absorption spectra were averaged and normalised to the phycoerythrobilin (PEB) absorption maximum (at 545 nm). By dividing the absorption peak height (at 495 nm) of phycourobilin (PUB) by the absorption peak height of PEB, PUB:PEB ratios were calculated (Waterbury (1986)).

To compare the ratios between the strains IMS101 and NIBB1067 with neglecting the effect of added nitrate, independent two-sample t-test was used. One-Way ANOVA followed by Tukey's Honestly Significant Difference test was used for statistical comparison of the PUB:PEB ratios between the four cultures (*T. erythraeum* IMS101 and NIBB1067, both under diazotrophic and non-diazotrophic conditions).

[1] For 1 liter of 10× concentration and 1M of NaCl: 58.44 g of NaCl, 6.23 g of $Na_2HPO_4 \cdot 2H_2O$ and 2.4 of $NaH_2PO_4 \cdot 2H_2O$

5.3 Fluorescence lifetime measurements

5.3.1 Time-resolved fluorescence spectroscopy

Time-resolved fluorescence spectroscopy is a technique which allows to detect events within a fluorophore's environment. Two types of measurements can be performed, one is measurement of the polarisation anisotropy decay, which monitors reorientation of the emission dipole during excitation (Millar (1996)). The other one, which we used, is measurement of the decay of fluorescence after excitation in order to determine the fluorescence lifetime, which is our intention. The theoretical principles for this technique and subsequent analysis using DAS are described in the section 4.1.

Before the measurements, samples were kept in a portable incubator with proper light and temperature conditions. Cell suspension was kept at 26 ° C and magnetically stirred during fluorescence measurement.

The measurements were done using the FluoTime 300 spectrometer (PicoQuant, Berlin, Germany). The excitation was provided with LDH-P-C-485 picosecond laser diode with maximum emission at about 481 nm. Repetition frequency was set to 10 MHz, instrument-specific excitation intensity settings was 10%, corresponding to about 16 μW radiant power. This setting was selected based on the requirement of sufficient signal intensity of about 10000 counts at maximum and as short as possible measurement time over the whole spectral range of interest that was set from 550 to 750 nm in 5 nm increments. A red-enhanced PMT cooled module was used as detector. The instrument response curve was acquired using colloidal silica (Ludox®) scattering sample. Global analysis of data to yield the lifetime components and their corresponding decay-associated spectra by iterative reconvolution was performed in the FluoFit software (PicoQuant). Quality of the fit was evaluated based on homogeneity of residual distribution and linearity of residual autocorrelation as provided by the analysis software.

5.3.2 Fluorescence-Lifetime Imaging Microscopy

Another technique based on the principles of fluorescence lifetime as described above is Fluorescence-Lifetime Imaging Microscopy (FLIM). Unlike time-resolved fluorescence spectroscopy, FLIM is used in order to obtain the spatial distribution of fluorescence lifetimes in the sample (Bücherl et al. (2014)). As a method based on displaying the fluorescence lifetimes, FLIM is independent of the fluorophore concentration, which makes it a powerful imaging technique (Peter et al. (2005)).

In general, the fluorescence lifetime can be determined either by using a frequency domain or time-domain approach (Marcu et al. (2014)), the latter was used in our measurements (TCSPC - see section 4.1.1).

For the measurements the samples were concentrated and placed on a piece of agar in a glass bottom Petri dish. Cells were kept at 26 ° C and 5% CO_2. FLIM measurements were performed using a Leica Stellaris confocal microscope equipped with FALCON module and white light laser (WLL). We utilised a water immersion objective 40× NA 1.1. Samples were illuminated with the 500 nm laser line using a pinhole size of 2.5 Airy units and SMD detector HyD X in the range of 560-700 nm. Pixel size was set to 284 nm and acquisition time to 1 min in order to acquire the desired number of photons. LAS X software was used for operating the microscope

and data analysis. Final FLIM images were generated using the fast-FLIM method according to Luis et al. (2019).

Two independent replicate experiments were performed.

5.4 Lugol staining

The solution of potassium iodide with iodine in water, known as Lugol's solution, is useful for staining starch in organic compounds. Cells containing starch, in the case of *Trichodesmium*, as glycogen, will turn blue-black after the formation of polyiodide chains, due to the iodine's reaction with the coil structure of the polysaccharide (Bailey and Whelan (1961)). Therefore previous studies have used it as an indicator of photosynthetically active cells.

In order to visualize diazocytes in *Trichodesmium* filaments, samples were left to stain with 2.5% v/v acidic iodine-potassium Lugol's solution for 2 hours. When staining the samples that were already measured by FLIM, the Lugol's solution was added directly to the sample placed under a piece of agar, and samples were imaged in a light microscope the following day.

5.4.1 Lugol's solution ideal concentration test

Samples for the concentration test were taken from all four types of batch cultures (*Trichodesmium* IMS 101 and NIBB 1067 both under diazotrophic and non-diazotrophic conditions). Two ml were taken from each sample and 2, 20 and 40 μl of Lugol's solution were added. The samples were left to stain for 2 hours and analysed with a light microscope.

6. Results

6.1 Pigments extraction

Measured absorption spectra of diazotrophic and non-diazotrophic filaments of *Trichodesmium* IMS101 and NIBB1067 are shown in Figure 6.1.

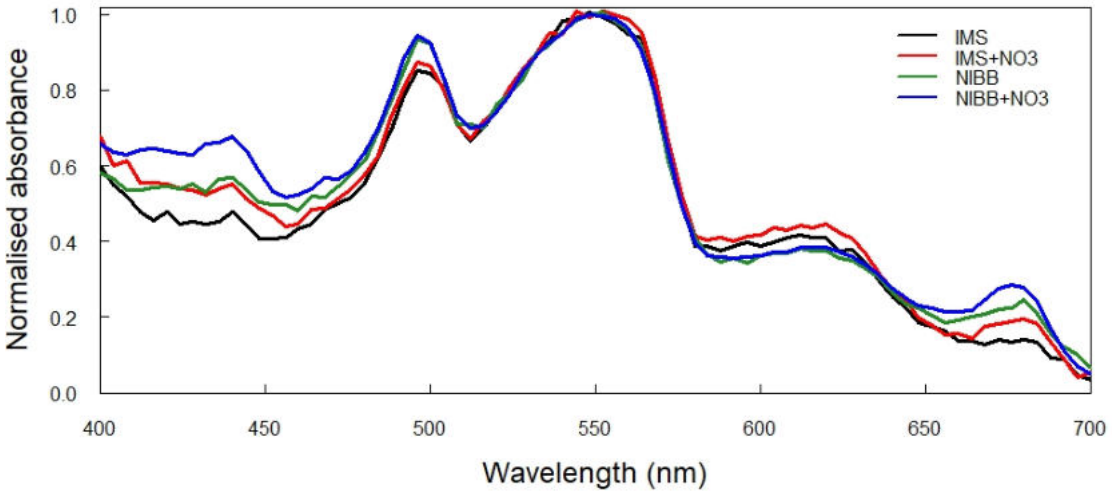

Figure 6.1: Absorption spectra of phycobiliproteins of *Trichodesmium* erythraeum strains. Absorption is normalised to the average in the vicinity (+/- 4 nm) of 545 nm. Each curve represents the average of three replicates of a given group.

The ratio of PUB:PEB pigment concentrations is statistically-significantly different between IMS101 and NIBB1067 strains ($t_{(14)} = -3.295; p = 0.005$)(see Fig. 6.2a) where the assumption of homogeneity of variance was met ($F_{(5)} = 1.249; p = 0.726$). The average PUB:PEB ratio in IMS101 strain is 0.884 and in NIBB1067 0.948.

When considering the effect of added nitrate, across all four groups, the assumption of homogeneity of variance is met (Bartlett $\chi^2_{(3)} = 3.259$; $p = 0.353$). We found a statistically-significant difference ($p < 0.05$) in PUB:PEB ratios ($f_{(3)} = 3.891; p = 0.037$). A Tukey test revealed that the ratio differs only between non-diazotrophic NIBB1067 and diazotrophic IMS101 ($p = 0.0406$)(see fig. 6.2b).

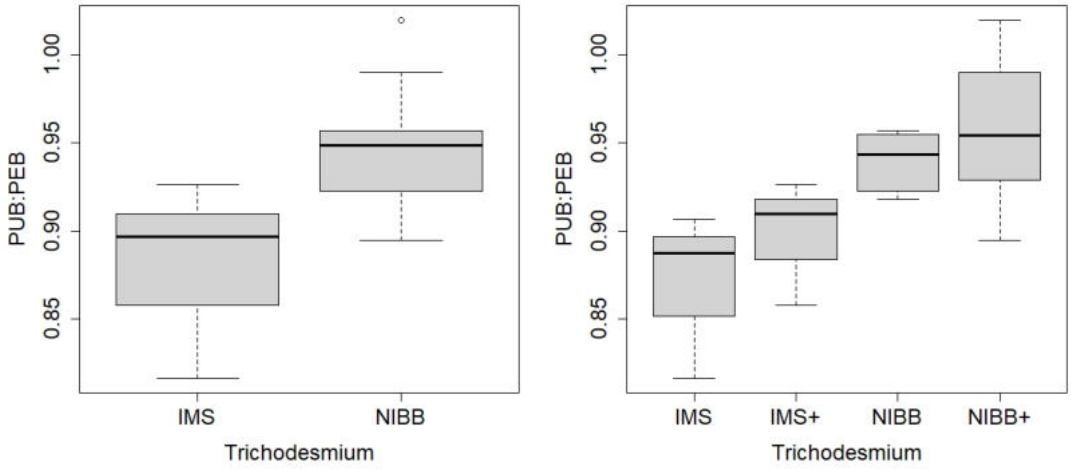

(a) (b)

Figure 6.2: Different phycourobilin (PUB) to phycoerythrobilin (PEB) concentration ratios (a) of the strains IMS101 and NIBB1067 with neglecting the effect of added nitrate. Their ratios are significantly different ($t_{(14)} = -3.295; p = 0.005$). And (b) PUB:PEB ratios of diazotrophic and non-diazotrophic (denoted as IMS+ and NIBB+) strains of IMS101 and NIBB1067. There is a statistically-significant difference between diazotrophic IMS101 and non-diazotrophic NIBB1067 ($p = 0.0406$).

6.2 Lugol staining

The staining patterns of *Trichodesmium* were sensitive to the concentration of Lugol's solution. As shown in Figure 6.3 using a non-specific amount of 2.5% Lugol's solution results in not clearly pronounced patterns as in Sandh et al. (2009), Sandh et al. (2011), Sandh et al. (2012).

For this reason, an ideal concentration test was performed and showed that the optimal amount of Lugol's stain is 10 μl/ ml of culture (Fig. 6.4b). When staining only with 1 μl/ml (fig. 6.4a), many filaments seem to have more than one diazocyte-like segment, which is not observed when staining with a higher concentration. On the other hand, when staining with 20 μl/ml (fig. 6.4c)), the unstained zones are hardly recognisable.

Figure 6.3: Not clearly pronounced diazocytes of *Trichodesmium* IMS101 due to insufficient amount of 2.5% Lugol's stain.

Looking at samples of *Trichodesmium* IMS101 stained by 10 μl of Lugol's stain per 1 ml of culture, diazocytes were distinguished

in 27/37 (i.e. 73 %) N_2-fixing filaments and 7/49 (i.e. 14 %) NO_3^--consuming filaments (Fig. 6.4d)).

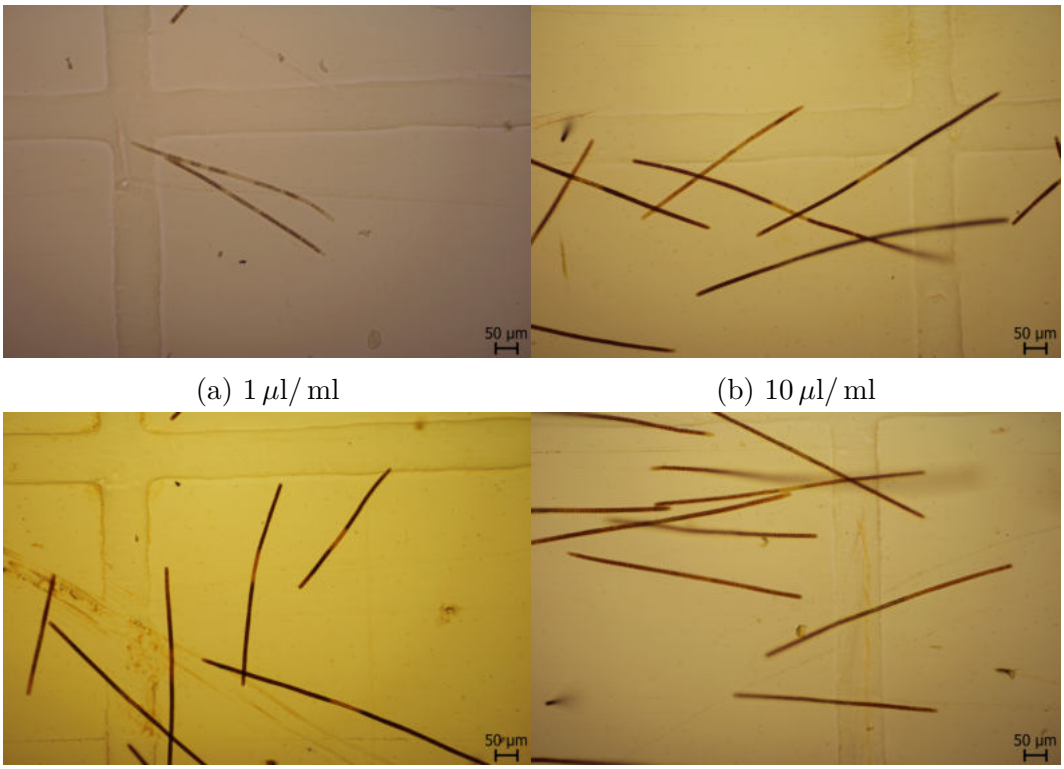

(a) 1 μl/ ml (b) 10 μl/ ml

(c) 20 μl/ ml (d) NO_3^--grown IMS, 10 μl/ ml

Figure 6.4: Samples of *Trichodesmium* IMS101 stained by Lugol's solution. Pictures a), b) and c) show the effect of the different amounts used for staining. Lugol's solution was added at midday and left to stain the cells for 2 hours. Picture d) shows a sample of NO_3^--grown *Trichodesmium* IMS101 stained by 10 μl of Lugol's stain per 1 ml of culture.

In the N_2-fixing *Trichodesmium* NIBB1067 (fig. 6.5a), one diazocyte-like segment was observed in $\sim$ 60 filaments. The NO_3^--consuming filaments of *Trichodesmium* NIBB1067 (Fig. 6.5b) did not show any pattern of diazocytes or any other unstained segments, however the filaments, both diazotrophic and non-diazotrophic, do not appear homogeneously stained as IMS101 does. Instead, there are light spots within the cells.

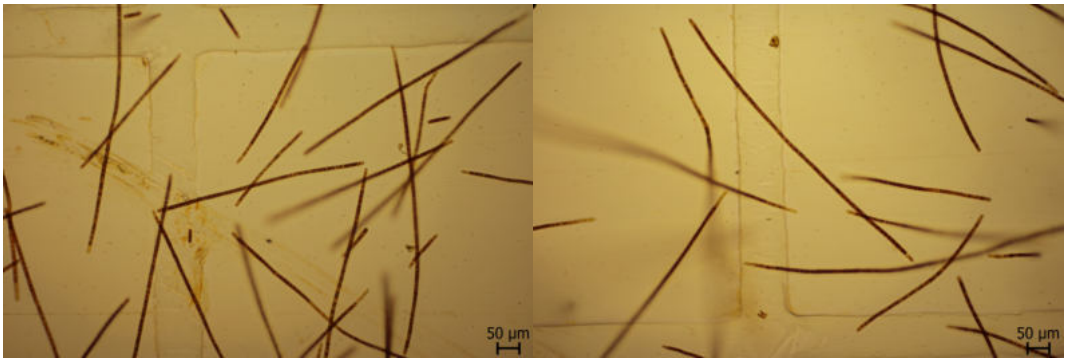

(a) N_2-fixing (b) NO_3^--consuming

Figure 6.5: Samples of N_2-fixing and NO_3^--consuming *Trichodesmium* NIBB1067 stained by 10 μl of Lugol's solution per ml of culture. The solution was left for 2 hours to stain.

6.3 Fluorescence lifetime measurements

6.3.1 Time-resolved fluorescence spectroscopy

Measurements of time-resolved fluorescence on suspensions of *Trichodesmium* were performed in the spectral range of 550-750 nm to gain insight into the energy transfer processes operating in the organism. The experiments were performed using 481 nm excitation. For convenience, in Fig. 6.6, we show the absorption spectrum of the cell suspension and also the steady-state emission spectrum acquired using the 481 nm excitation. As seen in this figure, the excitation used was mainly directed into the phycobilisome (PBS), namely its phycoerythrin (PE) component absorption.

The steady-state emission spectrum clearly shows a sharp peak around 575 nm that can be ascribed to PE. Other PBS components, phycocyanin and allophycocyanin can also be observed as indicated by peaks in the 630-670 nm region. The sharp feature around 680 nm most likely corresponds to chlorophyll-a. The minor peak at around 720 nm could be presumed to originate from red forms of Chl-a in the PS I complex.

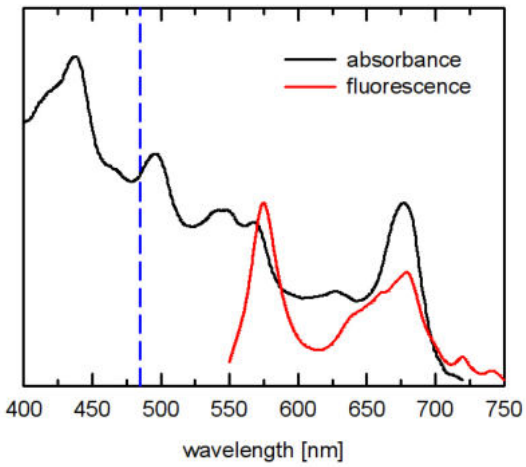

Figure 6.6: Absorbance spectrum of *Trichodesmium* IMS101 and its steady-state emission spectrum excited at 481 nm, the blue line indicates the excitation wavelength for the fluorescence experiment.

Examples of the time-resolved data are shown in Figure 6.7. In the left panel, we show kinetics of fluorescence at a selected wavelength corresponding to main features in the steady-state spectrum from Figure 6.6. Examples of time-resolved emission spectra at selected times are given in the right panel. One can readily observe that at all wavelengths, the signal contains a significant con-

tribution from slowly-decaying species. A brief inspection of the spectra in the right panel shows that PE emission at 575 nm is clearly present even after several nanoseconds after excitation, indicating presence of PE that does not transfer energy. This is in line with the presence of a prominent PE peak in the steady-state spectra.

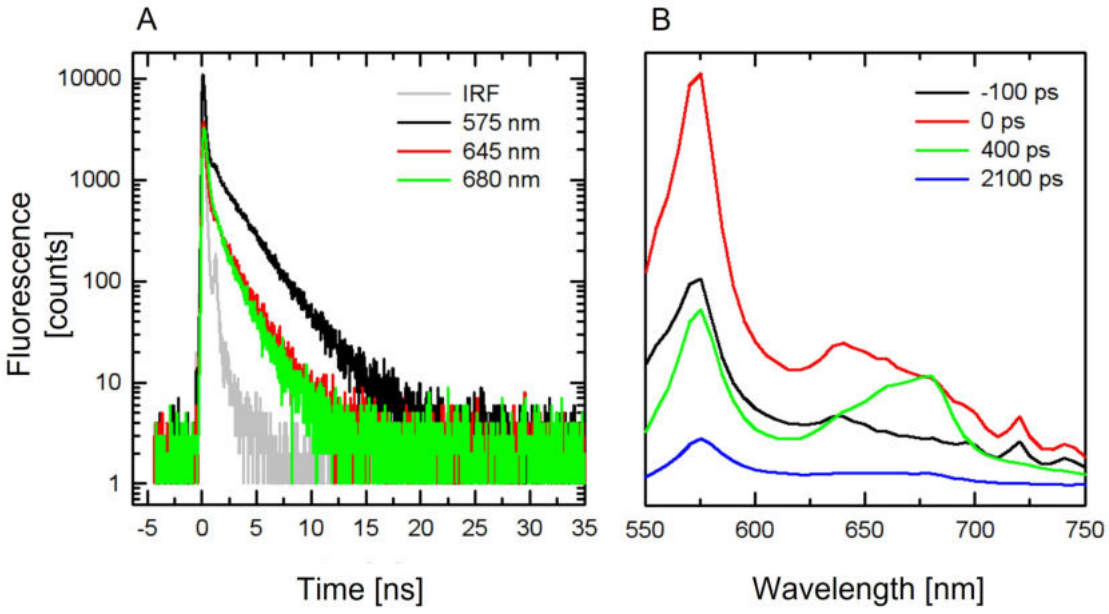

Figure 6.7: (A) shows selected fluorescence decays at several wavelengths acquired on *Trichodesmium* cell suspension. The instrument response is also shown (grey). Wavelengths are given in the legend. (B) shows emission spectra at selected times after excitation. The values in the legend are given relative to the maximum of the instrument response function.

The time-resolved fluorescence data were further globally analysed. The resulting DAS are shown in Fig. 6.8, which compares the data obtained from both nitrogen fixing and nitrogen replete ($+NO_3$) cultures. Data were normalised to a maximum of the emission spectrum at $t = 0$. Four components were sufficient to describe the data. As seen in Figure 6.8, dominant components were ∼70 ps (Fig. 6.8A) and 140 ps (Fig. 6.8B). The former DAS was positive in the region up to 650 nm and featured a prominent negative peak at ∼680 nm, hence, it can be interpreted as the component that characterises the overall energy transfer from PBS to Chl-a. It should be noted that this DAS contains a distinct peak at 575 nm, thus, it also includes the initial steps of energy transfer within the PBS that cannot be sufficiently resolved into individual steps of phycoerytrin-to-phycocyanin-to-allophycocyanin cascade. A small positive peak at around 720 nm can be observed in the fastest DAS. This can be interpreted as arising from excitation trapping in PSI RC. Given that the excitation used is likely to excite not only PBS, predominantly a PSII antenna system, but also carotenoids, it is likely that the data should also contain signals due to the direct excitation of PSI via its carotenoid complement.

The second major component, ∼140 ps (Fig. 6.8B) peaks at about 680 nm and lacks a major negative feature, hence, it can be interpreted as pure decay. Considering the position of the maximum, the most likely explanation is that this component mostly corresponds to energy equilibration and trapping within PSII.

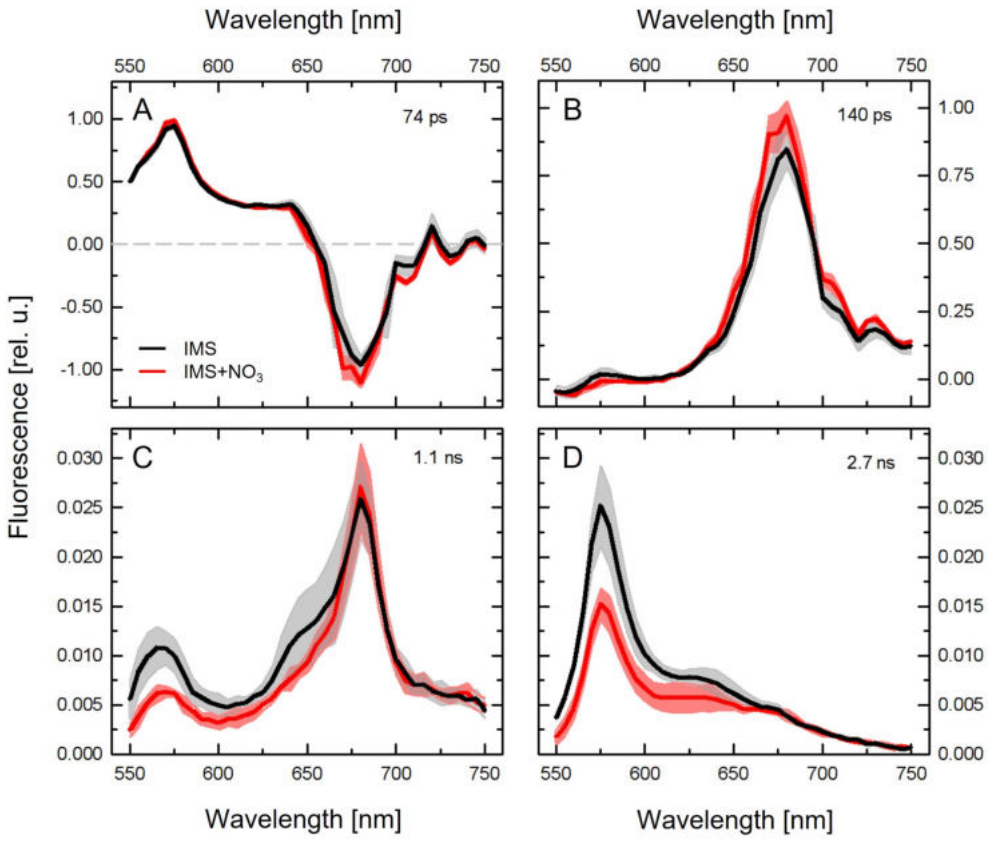

Figure 6.8: The Decay-Associated Spectra of N_2-fixing (IMS) and NO_3^--consuming (IMS + NO_3^-) *Trichodesmium* IMS101 culture showing four components of the fluorescence decay. (A) 74 ps component: mainly energy transfer from PBS to Chl-a. (B) 140 ps component: trapping within PSII. (C) 1.1 ns component: free PBS and Chl-a in closed RC. (D) 2.7 ns component: free PE. Lines correspond to averages of data from three biological replicates, the shaded area denotes ± standard deviation.

The following two components, which together correspond to a relative amplitude of less than 0.1, have lifetimes of ∼1 ns and 2.7 ns. The slowest of the two (Fig. 6.8D) can be readily ascribed to free PE based on its emission spectrum (Fujita and Shimura (1974)). The 1 ns component (Fig. 6.8C) aggregates contribution from free PBS, as evidenced by peaks around 570 and 650 nm, as well as chlorophyll-a around 680 nm.

Figure 6.8 shows that in the nitrogen-fixing culture the relative amount of PBS that does not transfer energy is about two times higher than in the NO_3^--supplied culture.

The data shown above using DAS can also be represented with average fluorescence lifetime. This representation using intensity-weighted average fluorescence lifetime τ_I (Fig. 6.9) clearly shows that the lifetime of PBS is longer in the sample grown under diazotrophic conditions (IMS) than in the one grown with NO_3^- (IMS+NO_3^-).

Stress conditions were simulated by exposing the suspension of NO_3^- supplied *Trichodesmium* IMS101 to high intensity light (2500μ mol) for seven minutes. Figure 6.10 shows that after applying high light to the cells, the relative number of uncoupled phycobilisomes increases by a factor of two.

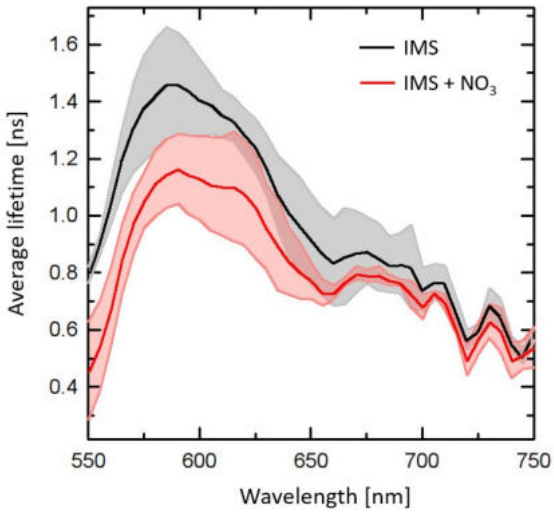

Figure 6.9: The intensity-weighted average fluorescence lifetime dependence of the wavelength of diazotrophic and non-diazotrophic (grown with NO_3^-) *Trichodesmium* IMS101. Lines correspond to averages of two experiments, the shaded area denotes ± standard deviation.

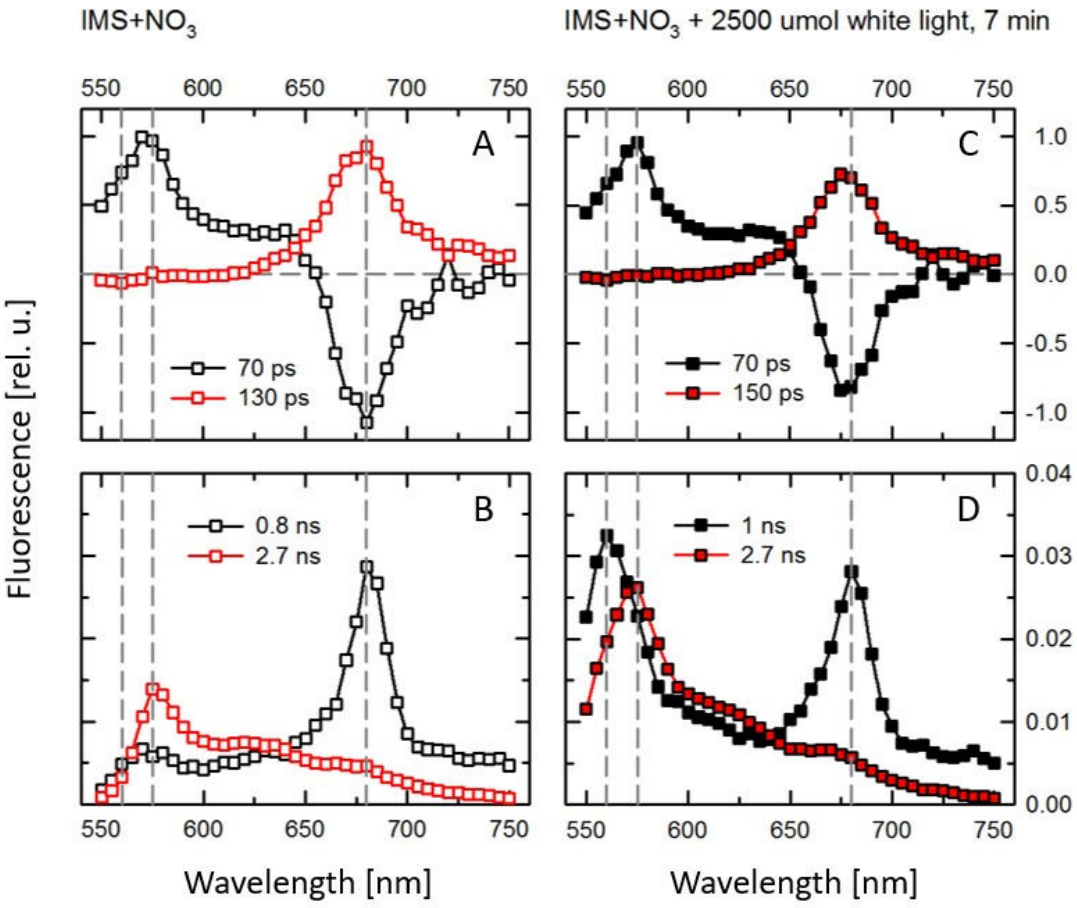

Figure 6.10: The Decay-Associated Spectra of NO_3^--consuming (IMS + NO_3^-) *Trichodesmium* IMS101 Panels (A) and (B) show DAS before, and panels (C) and (D) after applying high light (2500μ mol) for 7 minutes. In graph (D) the peaks of the ∼1 and 2.7 ns components have increased at 570 nm compared to the peaks in (B).

We measured the diel changes of the fluorescence lifetime of both diazotrophic and non-diazotrophic filaments. The average lifetimes for each time step are displayed in Figure 6.11. There are visible changes happening in the fluorescence lifetime of PBS during midday (565, 580 and 645 nm), whereas in Chl-a (680 nm) no significant change occurs. In the N_2-fixing *Trichodesmium* (IMS) the average lifetime increased during midday while in the NO_3^--consuming sample it decreased.

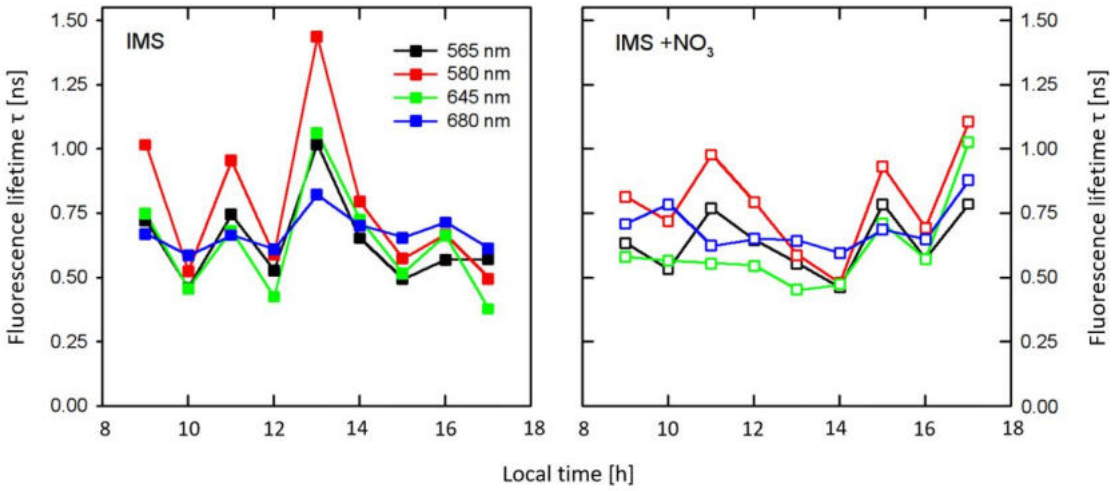

Figure 6.11: The diel changes of fluorescence lifetime of N_2-fixing (IMS) and not NO_3^- consuming (IMS + NO_3^-) *Trichodesmium* IMS101, with the light period starting at 7am.

6.3.2 Fluorescence-Lifetime Imaging Microscopy

In the first experiment, most of the cells had regular fluorescence lifetime ($\tau < 0.4$ ns). Cells with long fluorescence lifetime (≥ 1 ns) were observed in both N_2-fixing (IMS) and NO_3^- consuming (IMS + NO_3^-) filaments of *Trichodesmium* IMS101 (Fig. 6.12). This was observed in 23 % (7/30) of the N_2-fixing filaments and in 53% (10/19) of the NO_3^--consuming filaments. While in the N_2-fixing IMS101 it appeared in all different types of filaments, in the NO_3^--consuming samples, a segment with a long fluorescence lifetime appeared 7/10 times in a short filament.

In the NIBB1067 strain (Fig. 6.13), cells with long fluorescence lifetime appeared in 3% (1/35) (as a 2 cells segment) of N_2-fixing and in 63% (5/8) of NO_3^--consuming filaments, where 2/5 cases were short filaments.

In the second experiment, cells with a long fluorescence lifetime were found only in the samples of nitrogen-fixing *Trichodesmium*, both in IMS101 and in NIBB1067. Out of ∼100 filaments of *Trichodesmium* IMS101 analysed, eight contain a part with long fluorescence lifetime. In 7/8 cases it was an entire filament, in one of which there is also a single cell with a significantly longer lifetime than in the neighbouring cells. The remaining 1/8 has a diazocyte-like segment made of ∼10 cells. An unexpected phenomenon are segments with shorter fluorescence lifetime occurring in both N_2-fixing and NO^3-grown cyanobacteria. All these segments are approximately the same

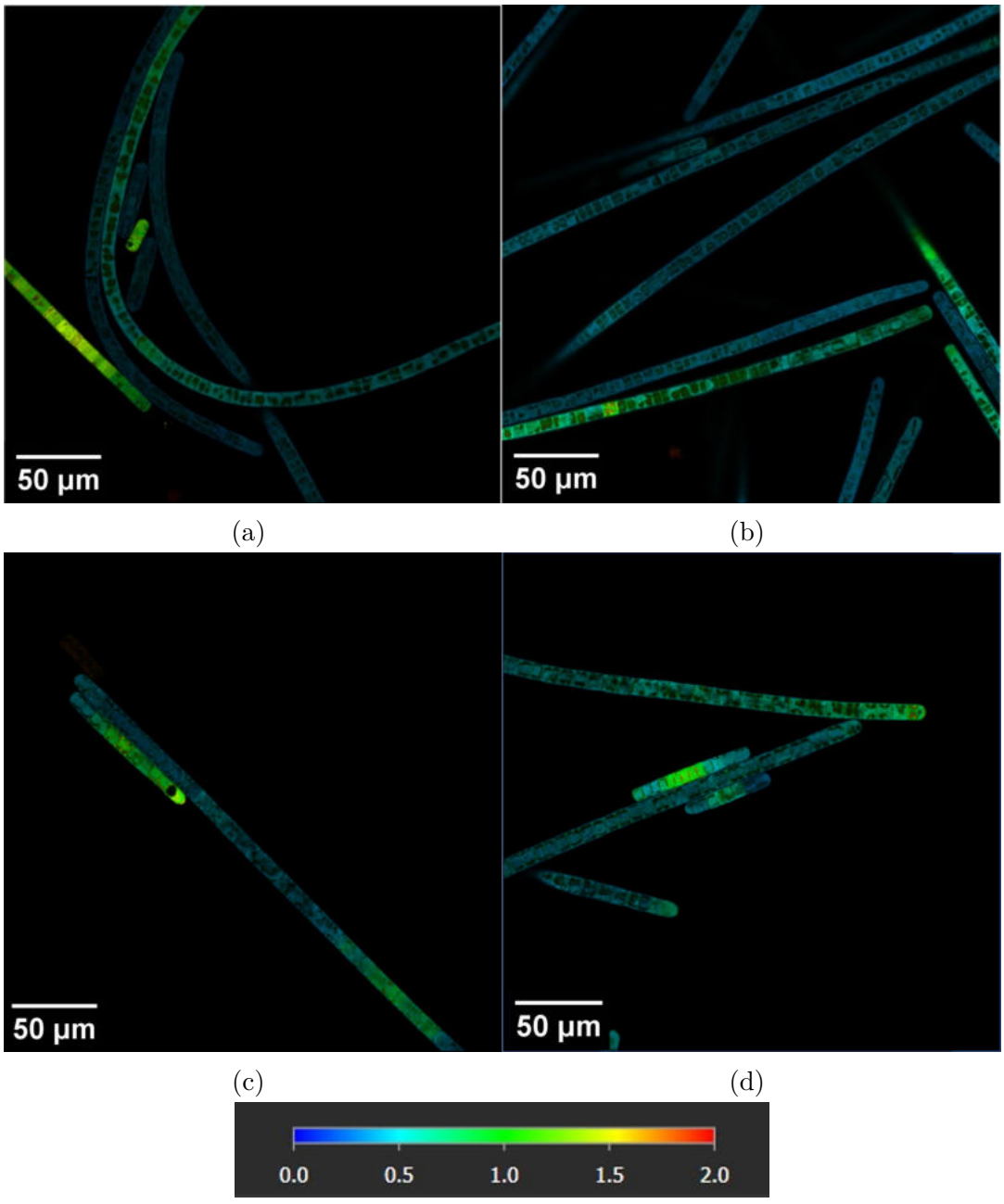

Figure 6.12: Panels a) and b) show fast-FLIM pictures of N_2-fixing filaments and c) and d) show NO_3^- consuming filaments of *Trichodesmium* IMS101 from the first experiment. Excitation at 500 nm, emission from 560 to 700 nm. The colour scale ranges from 0 to 2 ns. The scale bar applies to all the images.

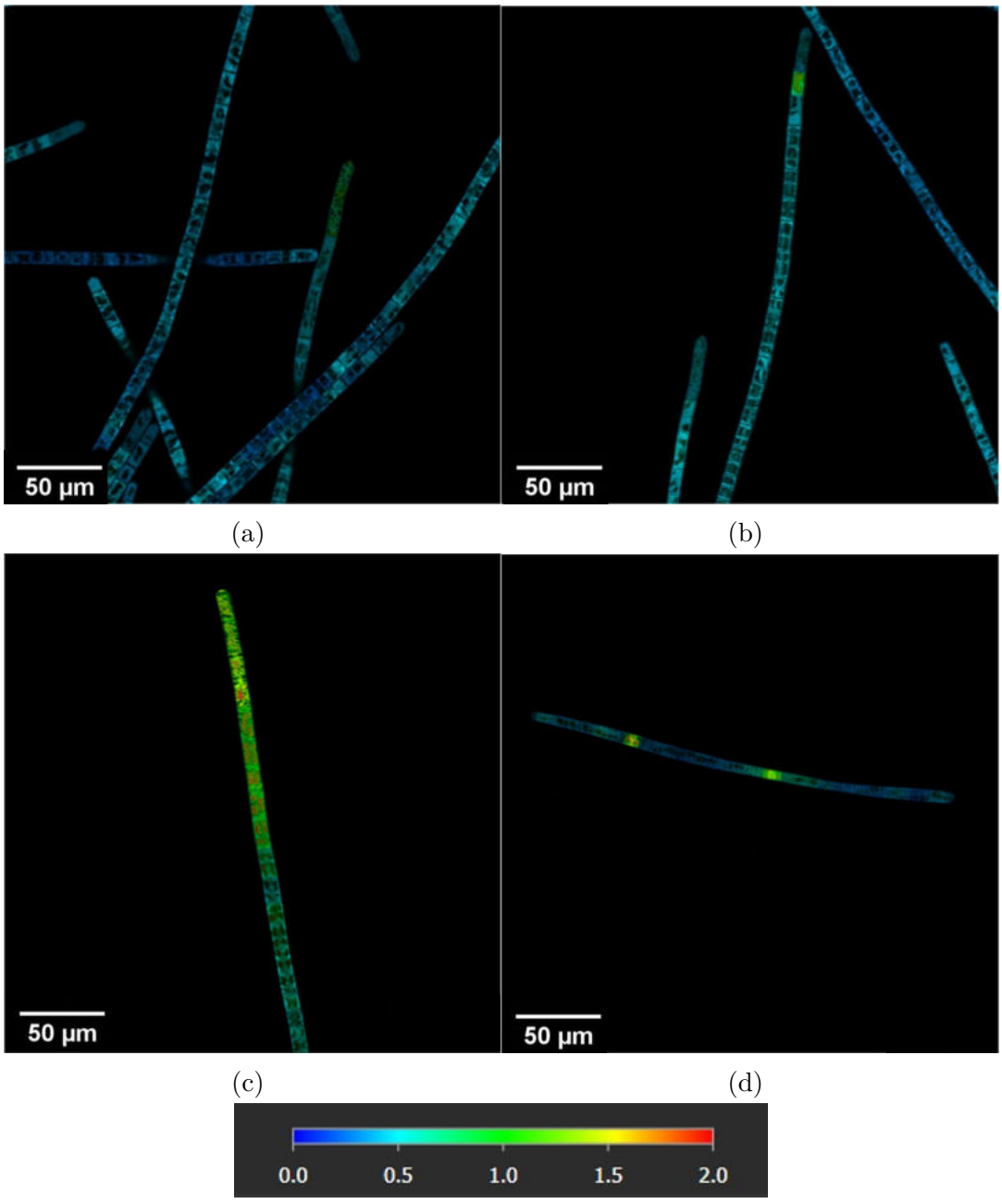

Figure 6.13: Panels a) and b) show fast-FLIM pictures of N_2-fixing filaments and c) and d) show NO_3^- consuming filaments of *Trichodesmium* NIBB1067 from the first experiment. Excitation at 500 nm, emission from 560 to 700 nm. The colour scale ranges from 0 to 2 ns.

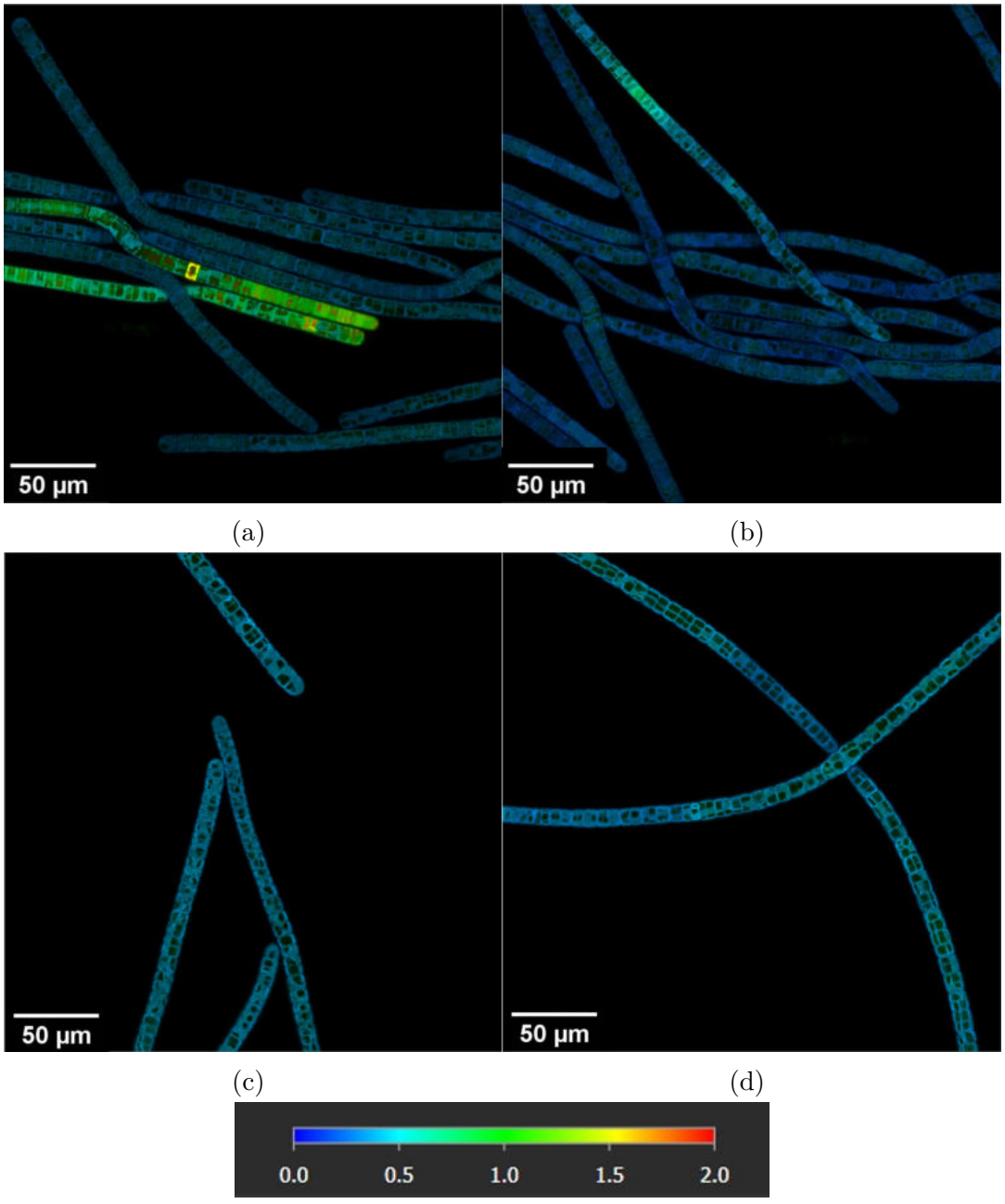

Figure 6.14: Panels a) and b) show fast-FLIM pictures of N_2-fixing filaments and c) and d) show NO_3^- consuming filaments of *Trichodesmium* IMS101 from the second experiment. Excitation at 500 nm, emission from 560 to 700 nm. The colour scale ranges from 0 to 2 ns.

length (∼15 cells) and are situated in the middle of the filament. This appeared in 7/100 filaments and 4/32 respectively.

As for the *Trichodesmium* NIBB1067 strain (Fig. 6.16, on page 38), in the samples under non-diazotrophic conditions, no cell with a significantly higher fluorescence lifetime was observed. In the diazotrophic samples, there were 9% (5/58) filaments with a segment of cells with longer fluorescence lifetime. Out of the five cases, three have fluorescence lifetime higher than 1.5 ns: one is a short filament starting to dissolve, another is a filament's tip and the last one is a single bright cell. The remaining two cases with a lifetime ~ 1 ns are segments made of $\sim$ 5-8 cells. The phenomenon of short fluorescence lifetime appeared both in the N_2-fixing and NO_3^--consuming filaments, however, compared to IMS101, here the segments length and position are not uniform among the filaments. Another phenomenon observed with a high frequency is a special morphology of 5-10 cells at the end of the filaments ("granulated tips", Fig. 6.15). They seem to have many gas vesicles, low fluorescence intensity and slightly longer fluorescence lifetime. Granulated tips appeared in 33% (12/36) visible tips[1] of N_2-fixing filaments and in 57% (17/30) visible tips[2] of NO_3^--consuming filaments.

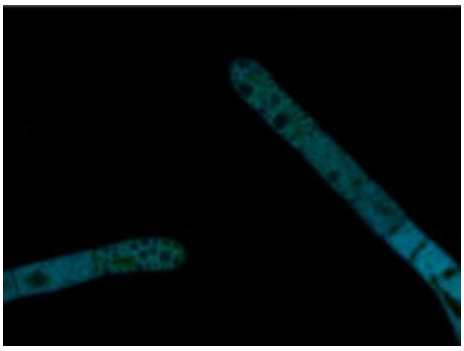

Figure 6.15: Fast-FLIM picture of the end cells of *Trichodesmium* NIBB1067 with special morphology of "granulated tips".

[1]In the measured images there are only three filaments that are visible in their full length with both ends (i.e. 3 × 2 tips). The remaining filaments are only partially visible. In total there are 30 filaments with 1 visible tip + 3 filaments with 2 visible tips = 33 filaments and 36 tips

[2]There are 2 filaments visible with both tips and 26 filaments with one tip, i.e. 28 filaments and 30 tips.

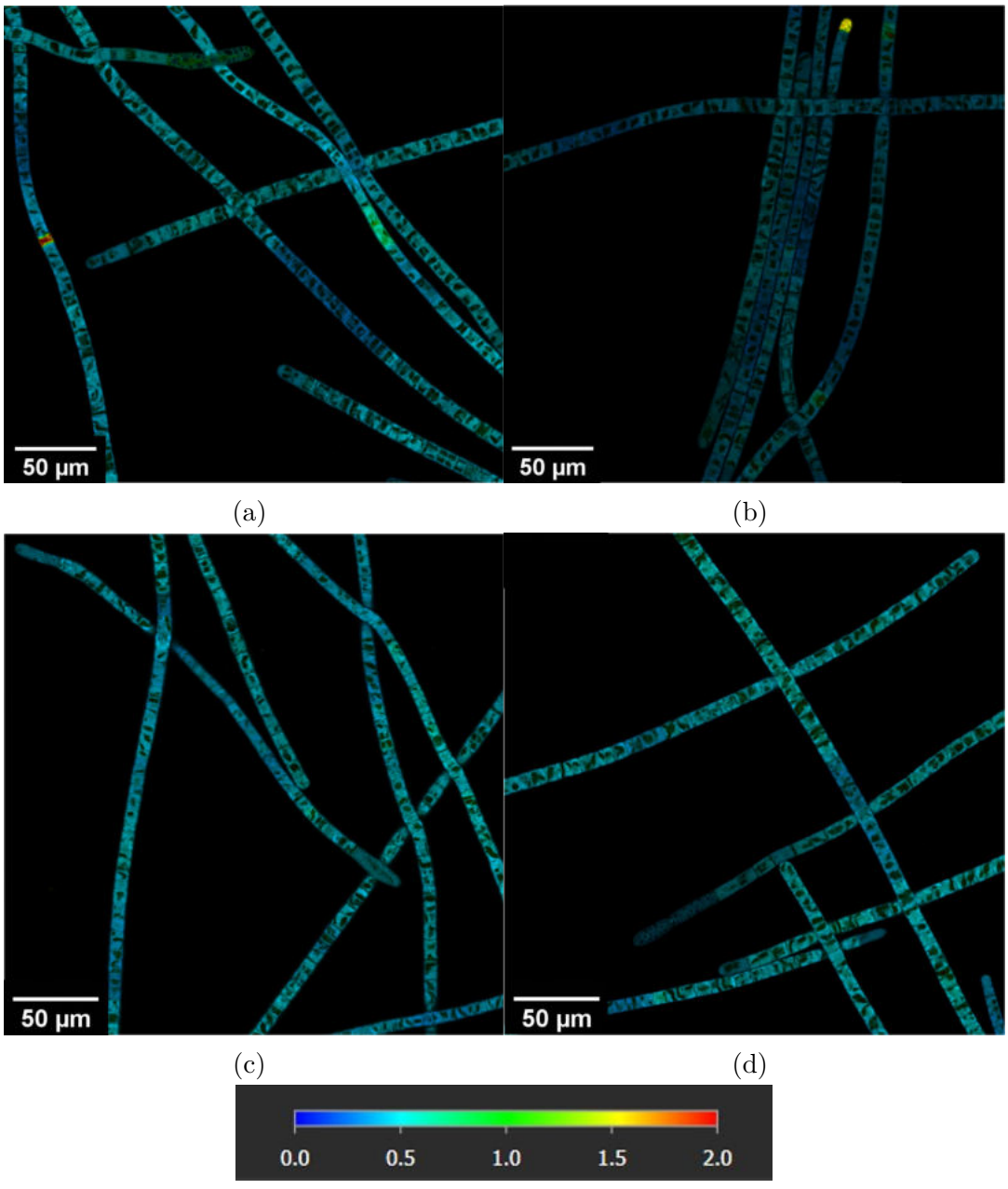

Figure 6.16: Panels a) and b) show fast-FLIM pictures of N_2-fixing filaments and c) and d) show NO_3^- consuming filaments of *Trichodesmium* NIBB1067 from the second experiment. Excitation at 500 nm, emission from 560 to 700 nm. The colour scale ranges from 0 to 2 ns.

Comparison with Lugol's stain

The Lugol-stained samples, allow a direct comparison between the fluorescence and the diazocyte patterns, with which further conclusions about other ongoing cell processes can be drawn. Based on this comparison, we divided the observed patterns of *Trichodesmium* IMS101 into seven different types, which are summarised in table 6.1. In the diazotrophic samples, in 10 out of 100 filaments, there was an unstained segment.[3]

Type	Lugol	FLIM	Morph	Cell no	Freq N_2	Freq NO_3^-
1 Normal	stained	regular	regular	whole fil	82/100	28/32
2 Diazocyte	light zone	bright	regular	∼15	1/100	0/32
3 Bright cell	stained	bright	regular	1-2	1/100	0/32
4 Bright fil	unstained/ partly/ stained	bright	regular	whole fil	7/100	0/32
5 Short τ	light zone	dark	thin	∼15	7/100	2/32
6 Short fil	unstained	bright	short f	whole fil	1/100	0/32
7 Unstain.	light zone	regular	regular	∼10	3/100	2/32

Table 6.1: Table summarising the seven different Lugol staining-FLIM patterns observed. The "Lugol" column describes how the filament was stained by the Lugol's solution, where "light zone" means a diazocyte-like segment. The "FLIM" column characterises the appearance of filaments in fast FLIM pictures. Regular: $\tau \approx 0.2 - 0.4$ ns, bright: $\tau > 0.4$ ns and dark: $\tau < 0.2$ ns. The following columns describe the morphology of each type, how many cells are involved and how often certain types appeared in N_2-fixing and NO_3^--consuming samples of *Trichodesmium* IMS101. The bright cell and the short filament appeared within the group of bright filaments, therefore they were counted twice and the numbers do not add up to 100.

The tips unstained by Lugol often correspond to morphologically different cells (the tip cells are smaller and have slightly lower intensity than the stained, regular tips). For this reason, they are considered a separate type from the unstained segments in the middle of the filaments.

In the following paragraphs, one example of each type is shown. The rest of the pictures is included in the attachment A.1.

The type 1 ("normal") is when a fully Lugol-stained filament corresponds to a regular (< 0.3 ns) fluorescence lifetime. With an occurrence of 82/100 (82 %) in N_2-fixing filaments of IMS101 and 28/32 (88 %) in NO_3^--consuming samples, this was the most frequently observed type.

[3]The filaments are usually not visible in the whole length, only the visible segments were counted.

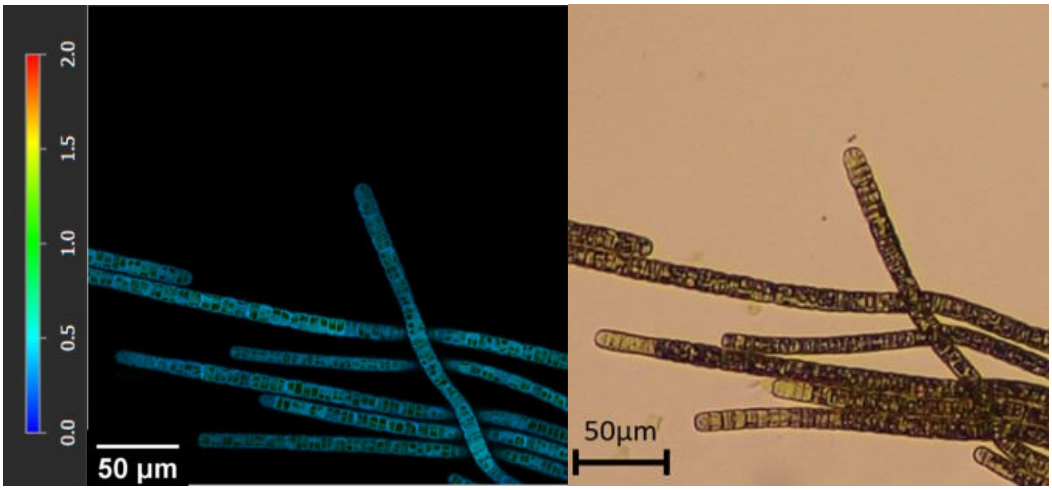

(a) (b) fast-FLIM (c) Lugol staining

Figure 6.17: Type 1 "normal". Comparison of pictures of the same sample of N_2-fixing *Trichodesmium* IMS101 (b) from FLIM and (c) after staining with Lugol's solution. There are neither segments with irregular fluorescence lifetime nor segments unstained with Lugol, except for the tips. (a) The colour scale ranges from 0 to 2 ns.

In line with the hypothesis stating that the segments with active nitrogenase will have a longer fluorescence lifetime, we call a pattern "diazocyte" (type 2) (Fig. 6.18) in the case when an unstained segment made of $\sim$ 15 cells corresponds to a bright segment in the fast FLIM picture (i.e. a segment with $\sim$ 1 ns fluorescence lifetime). This was observed only in 1/100 N_2-fixing filaments of IMS101.

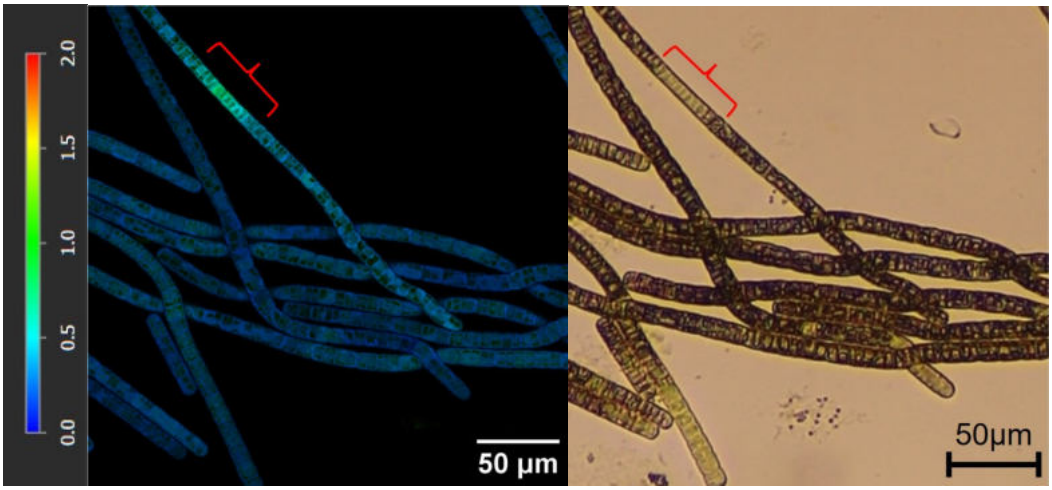

(a) (b) fast-FLIM (c) Lugol staining

Figure 6.18: Type 2 "diazocyte". Comparison of pictures of the same sample of N_2-fixing *Trichodesmium* IMS101 (b) from FLIM and (c) after staining with Lugol's solution. The red lines indicate the same segment, considered as a diazocyte. (a) The colour scale ranges from 0 to 2 ns.

The type 3 ("bright cell") (Fig. 6.19) as introduced by Küpper et al. (2009), stands for a single cell having a $\pm$ 2 times higher fluorescence intensity than the

adjacent cells. However, this cell was fully stained and showed no difference under Lugol.

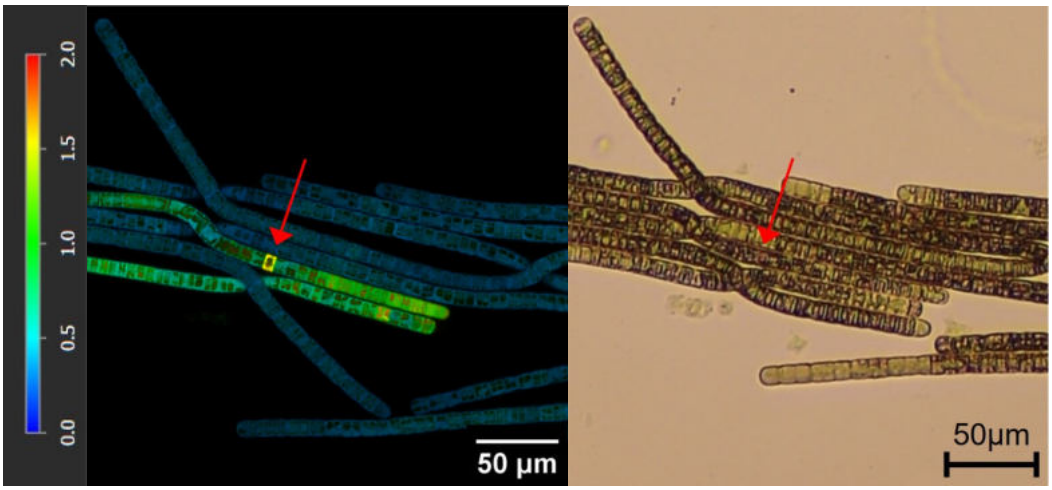

(a) (b) fast-FLIM (c) Lugol staining

Figure 6.19: Type 3 "bright cell". Comparison of pictures of the same sample of N_2-fixing *Trichodesmium* IMS101 (b) from FLIM and (c) after staining with Lugol's solution. The red arrows indicate the same cell, considered a bright cell. (a) The colour scale ranges from 0 to 2 ns.

While a single bright cell appeared only in 1/100 N_2-fixing filaments a whole bright filament (type 4) (Fig. 6.20) appeared in 8/100 N_2-fixing filaments analysed. These are the filaments with a fluorescence lifetime > 0.3 ns, appearing brighter than the majority of filaments in fast FLIM images. The Lugol staining in these filaments was not uniform.

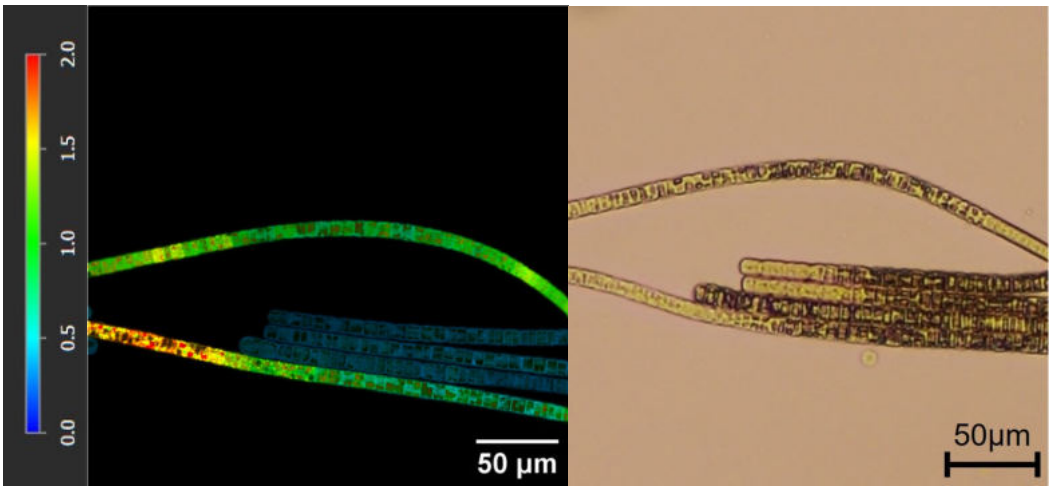

(a) (b) fast-FLIM (c) Lugol staining

Figure 6.20: Type 4 "bright filaments". Comparison of pictures of the same sample of N_2-fixing *Trichodesmium* IMS101 (b) from FLIM and (c) after staining with Lugol's solution. (a) The colour scale ranges from 0 to 2 ns.

The segments with shorter lifetime (type 5), which appear dark in the fast FLIM images, correspond to unstained diazocyte-like segments (Fig. 6.21). These seg-

ments are also distinguished by their morphology. A paired-samples t-test was conducted[4] to compare the width of cells with short and regular fluorescence lifetime. There was a significant difference in the widths of short lifetime cells ($M = 8.2\,\mu m$, $SD = 0.8\,\mu m$) and regular lifetime cells ($M = 9.2\,\mu m$, $SD = 1.1\,\mu m$), t_{17}=8.9, $p = 8.43 \cdot 10^{-8}$. These results suggest that cells with short fluorescence lifetime are thinner than regular cells.

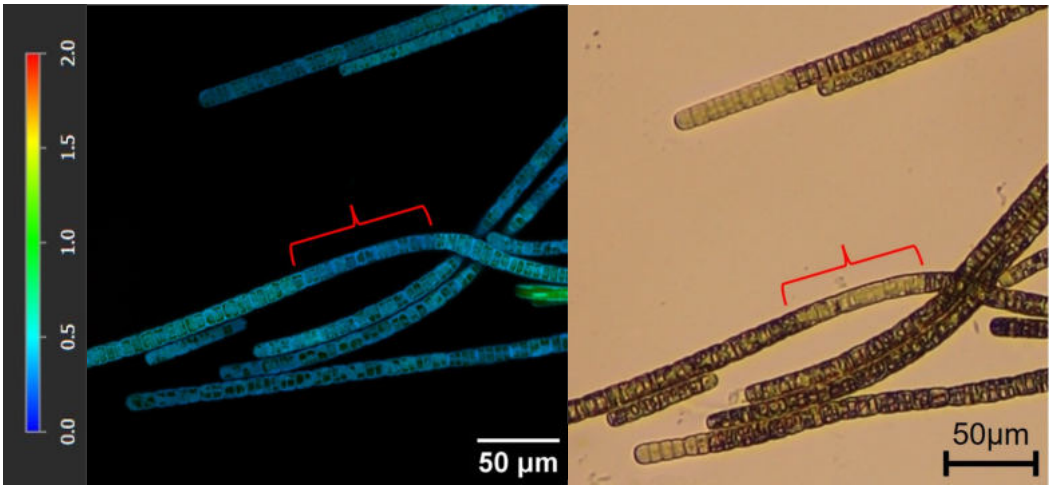

(a) (b) fast-FLIM (c) Lugol staining

Figure 6.21: Type 5 "short τ". Comparison of pictures of the same sample of N_2-fixing *Trichodesmium* IMS101 (b) from FLIM and (c) after staining with Lugol's solution. The red lines indicate the same segment. (a) The colour scale ranges from 0 to 2 ns.

Due to the results from the first experiment, short filaments unstained by Lugol's solution, also belonging to the bright filaments, are considered as a separate type (type 6) (Fig. 6.22). Nevertheless, for the first experiment, there is no comparison with stained filaments. In the second experiment this type was only observed once in the N_2-fixing filaments. However, two short filaments with a regular lifetime and full Lugol staining appeared.

[4]Each filament containing a segment with short lifetime was measured at three places within the segments and at three random places outside the segment.

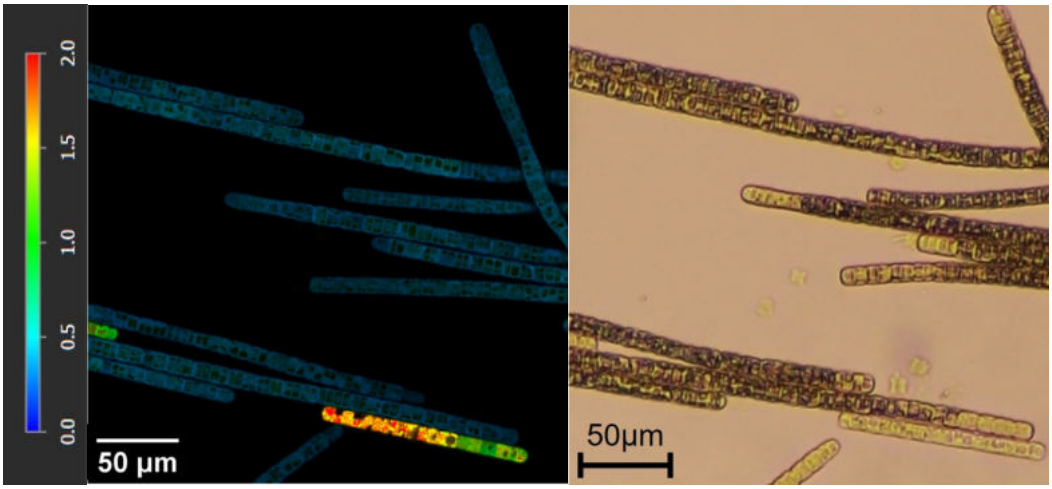

(a) (b) fast-FLIM (c) Lugol staining

Figure 6.22: Type 6 "short filament". Comparison of pictures of the same sample of N_2-fixing *Trichodesmium* IMS101 (b) from FLIM and (c) after staining with Lugol's solution. (a) The colour scale ranges from 0 to 2 ns.

The last cell type (type 7) belongs to the unstained segments that do not match a specific FLIM pattern (Fig. 6.23). This was observed three times (3 %) in the N_2-fixing and two times (6 %) in the NO_3^--grown filaments.

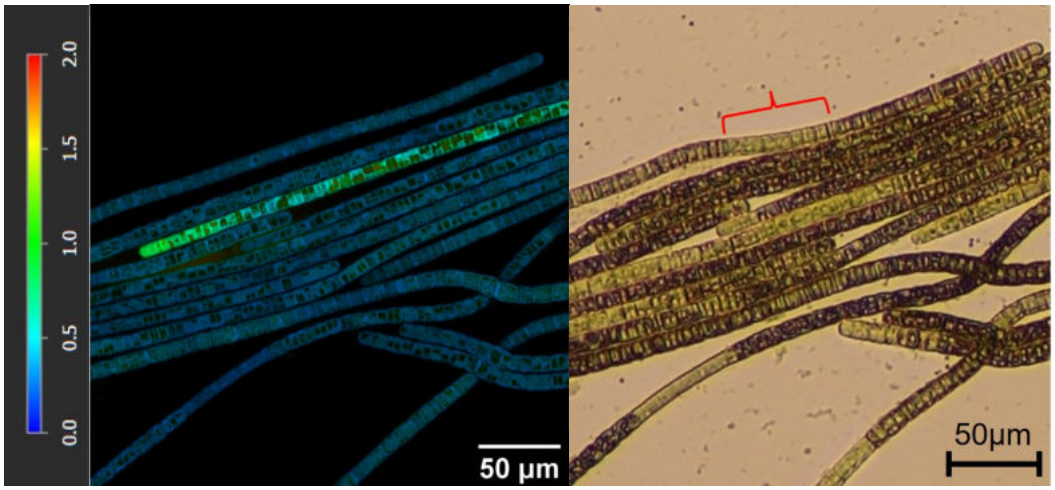

(a) (b) fast-FLIM (c) Lugol staining

Figure 6.23: Type 7 "unstained". Comparison of pictures of the same sample of N_2-fixing *Trichodesmium* IMS101 (b) from FLIM and (c) after staining with Lugol's solution. The red line indicates the unstained segment, which does not show any specific FLIM pattern. (a) The colour scale ranges from 0 to 2 ns.

We were not able to localise the stained filaments from the NIBB1067 samples in the light microscope. However, Figure 6.24 show filaments from the same samples that were used for FLIM measurements. In the N_2-fixing sample (Fig. 6.24a), there are no visible patterns of any diazocytes or any other special phenomenon, except for the granulated tips that appear unstained. In the non-diazotrophic sample, on the left side of Figure 6.24b, there is one fully unstained segment of cells, suggesting the presence of a diazocyte.

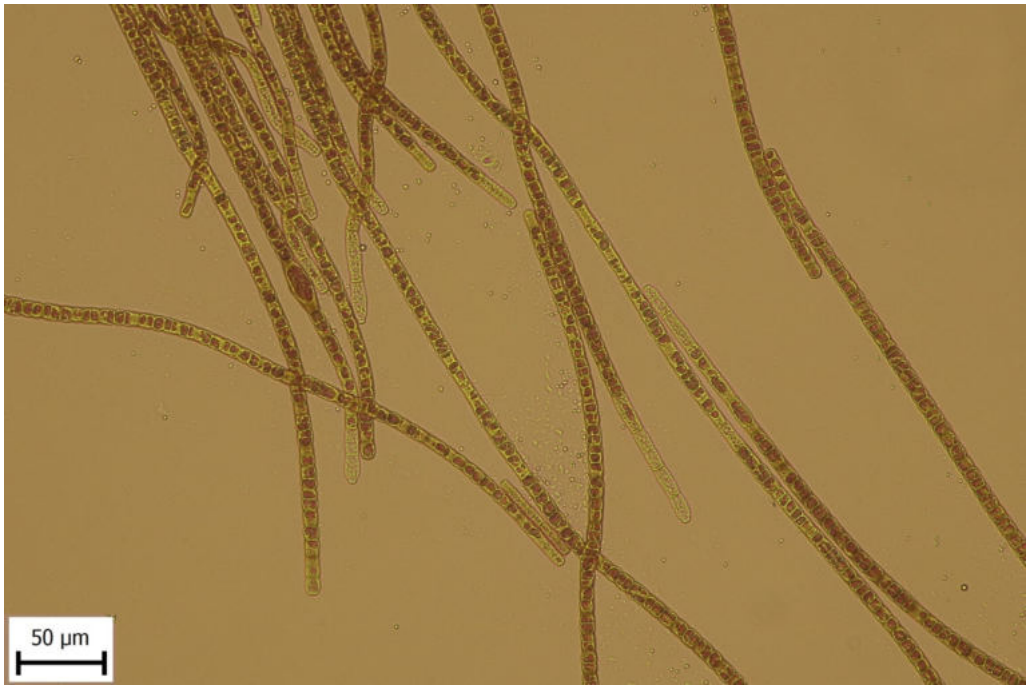

(a) N_2-fixing

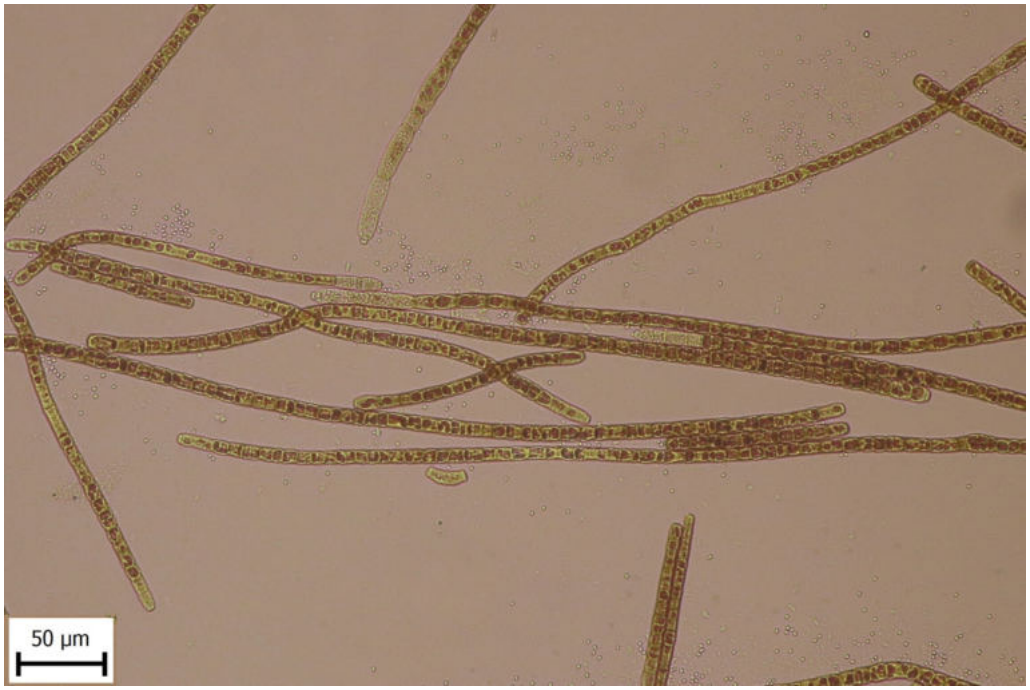

(b) NO_3^--consuming

Figure 6.24: Samples of (a) N_2-fixing and (b) NO_3^--consuming *Trichodesmium* NIBB1067 stained by Lugol's solution after being used for a FLIM measurement.

Stains IMS101 (Fig. 6.25a) and NIBB1067 (Fig. 6.25b) show a different Lugol staining pattern. While in IMS101 the stained cells look homogeneously stained, the staining in NIBB1067 cells looks patchy.

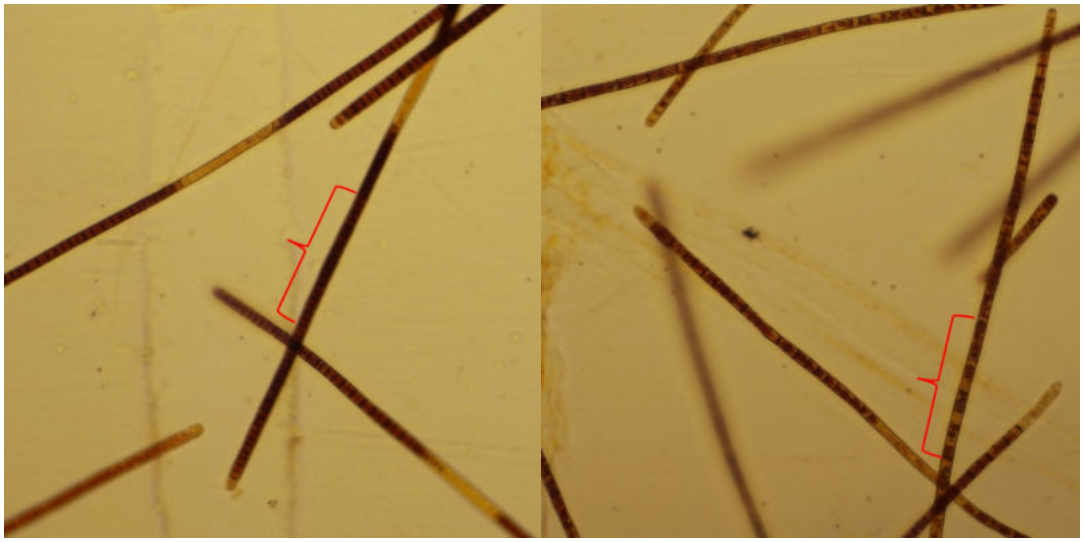

(a) N_2-fixing IMS101 (b) N_2-fixing NIBB1067

Figure 6.25: Comparison of the Lugol staining patterns of the diazotrophic *Trichodesmium* IMS101 and NIBB1067. The red lines indicate sections where the difference is most obvious.

Time evolution of fluorescence lifetime

One-hour observations of N_2-fixing *Trichodesmium* IMS101 showed that sections of cells with a long fluorescence lifetime break and disappear without returning to the stage with short fluorescence lifetime.

As shown in Figure 6.26, after the first time point i.e. 30 minutes (6.26b), the cells with the highest fluorescence lifetime ($\sim$ 2 ns) dissolved and disappeared. The rest of the cells remained the same, and no return to regular fluorescence lifetime was observed. In the next time point (after 1 h; Fig. 6.26c), no more cells disappeared, but one filament broke, despite the fact that the lifetime seemed to be regular.

Figure (6.26d) shows the same sample after staining with a Lugol's solution. There are 6 unstained segments: 4 unstained diazocyte-like segments, one unstained short filament and an unstained broken end of the middle filament. The segments appearing with long fluorescence lifetime in the fast-FLIM pictures are marked by red arrows and the ones marked by yellow arrows appear with short fluorescence lifetime in the fast-FLIM images.

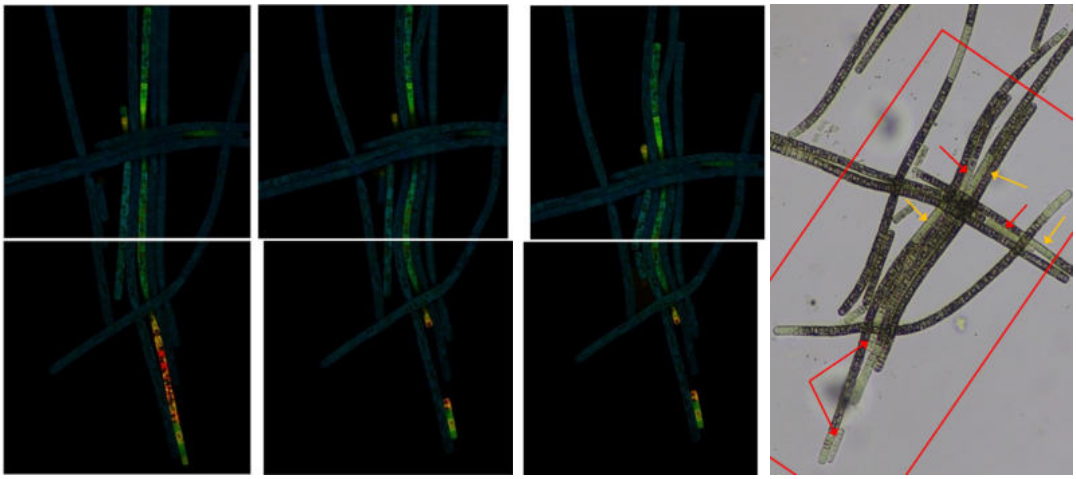

(a) 0 min (b) +30 min (c) +1 h (d) The same sample stained with Lugol's solution

Figure 6.26: Time evolution of fluorescence lifetime of a colony of *Trichodesmium* IMS101 measured by FLIM over one hour. Between timepoints a), b) and c) the colony was kept for 30 minutes at 26° C under a table lamp, with no measurement. d) shows the same sample stained with Lugol's solution immediately after finishing the FLIM measurements and examined with a light microscope. The red rectangle indicates the area captured by FLIM. The red and yellow arrows indicate segments with longer and shorter fluorescence lifetimes, respectively.

7. Discussion

7.1 *Trichodesmium* IMS101

Overall, differences between the N_2-fixing and NO_3^--consuming filaments were observed in all the measurements performed. The filaments grown under diazotrophic conditions showed segments unstained by Lugol, longer average fluorescence lifetime and more uncoupled PBS in time-resolved fluorescence spectroscopy and various patterns of cells with long fluorescence lifetime in FLIM. In contrast, the filaments grown under non-diazotrophic conditions were mostly fully stained by Lugol, had shorter average fluorescence lifetime and less uncoupled PBS in time-resolved fluorescence spectroscopy, and in FLIM only the segments with shorter τ were observed.

7.1.1 Lugol staining

According to several studies, *Trichodesmium* sequester the nitrogenase enzyme into specialised cells, diazocytes, which were identified using immunolabelling-TEM analyses (Bergman and Carpenter (1991), Fredriksson and Bergman (1997), Berman-Frank et al. (2001b)). These detected nitrogenase-containing cells and groups of lighter cells appearing after staining the *Trichodesmium* filaments by Lugol's stain have an almost identical positioning (Sandh et al. (2009)). In our experiments, unstained segments were found predominantly in filaments grown under diazotrophic conditions, while filaments grown under non-diazotrophic conditions, with NO_3^-, appeared homogeneously stained. Hence, we believe that the segments' appearance indeed correlates with nitrogen fixation and they can be considered diazocytes. Moreover, this conclusion is supported by the earlier findings that the nitrogenase expression in IMS101 is restricted to a subset of cells in a diazocyte-like form (Berman-Frank et al. (2001b)). Owing to this, Lugol staining works as a good and simple indicator of N_2-fixation in cells, and a direct comparison with staining patterns can help to decide whether any other observed phenomena relate to N_2-fixation.

Diazocytes (unstained segments), however, do not appear in 100% of the filaments which indicates that there must be extracellular transport of nitrogen between filaments. Extracellular transfer was studied by Mulholland et al. (2004), Mulholland and Capone (2009).

7.1.2 Time-resolved fluorescence spectroscopy

For fitting the measured decay, we had to decide, how many fit components to use. The most important criterion for deciding was the shape of the fit residuals which is best illustrated graphically, as in the figure 7.1. Here, both panels show the same TCSPC dataset, in the left panel the data were fit with three-exponential model. One can see that in the simpler model, the residuals exhibit a pronounced trend (a slowly oscillating pattern), rather than being evenly distributed around zero, and in this particular case, the mismatch between the model and the data can be directly observed in the longer decay times. In contrast, application of the four-component model produced residuals free of any trend, as shown in the right panel, this model was thus applied to all data.

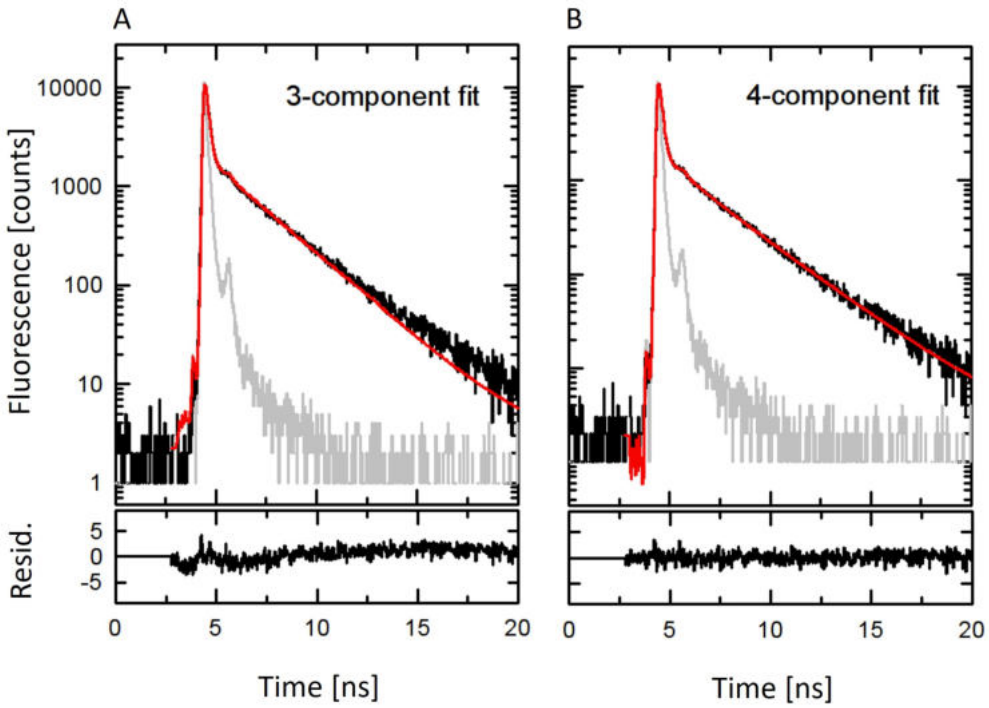

Figure 7.1: A TCSPC dataset fitted with (A) 3 components and (B) 4 components, respectively. Lower panels show the fit residuals. The residuals belonging to the three-exponential model oscillate, whereas the residuals of the four-exponential model are almost perfectly linear. Upper panels: black=data; red=fit; grey=IRF.

Figure 7.2 shows an example of TCSPC traces recorded at three different wavelengths and the corresponding four components fit and its residuals.

The fastest component with time of about 70 ps corresponds perfectly to the PBS-to-PSII transfer component observed in whole cells of the cyanobacterium *Synechococcus* WH7803 (Acuña et al. (2018)). For the second component, we can refer to the same article, where they observed a ∼130 ps component and interpreted it as predominantly due to PSII. In Grabowski and Gantt (1978) the lifetime of PE corresponds exactly to our fourth component of ∼2.7 ns.

In order to ensure that the peak at 680 nm in the 1 ns component is caused by chl-a and not by terminal emitters APC, DCMU (3-(3,4-dichlorophenyl)-1,1-dimethylurea) was used. DCMU, a specific inhibitor of photosynthesis, replaces the plastoquinone binding site of Q_B of PSII RC. This means that Q_A will accumulate in the light, and the charge separation will be followed by the recombination, and the energy will return to the antenna. If the peak indeed belongs to chl-a, a pigment present in the PSII RC, its relative amplitude in DAS will increase. For this reason, 50 μl of 6.25 μM DCMU was added to 2 ml of diazotrophic *Trichodesmium* IMS101. The sample was left in the dark for 5 min before measurement. The addition of DCMU resulted in a high narrow peak (Fig. 7.3) confirming our presumption.

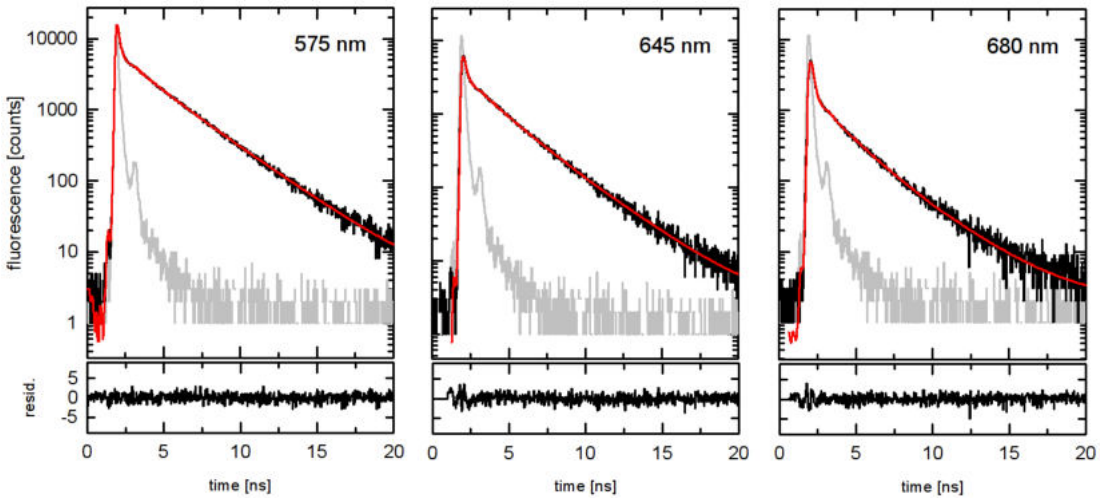

Figure 7.2: Example of TCSPC traces acquired on suspension of *Trichodesmium* IMS101 cells. Plots show data recorded at three different wavelengths, as indicated in the legends. Upper panels: black=data; red=fit (four components - exponentials); grey=IRF. Lower panels show the fit residuals.

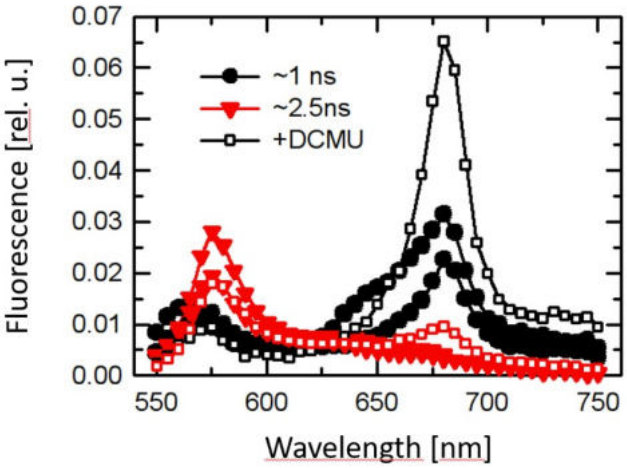

Figure 7.3: Adding DCMU to the sample has increased the fluorescence at 680 nm which indicates the presence of Chlorophyll-a.

In the graph showing the average fluorescence lifetime (Fig. 6.9), the standard deviation is relatively high in the area up to 670 nm. This is because the lifetime values in the first and second experiments did not correspond in this area, which follows that phycobilisomes are the flexible part of the photosynthetic apparatus. However, for both cases, the lifetime τ_I of PBS is longer in the sample grown under diazotrophic conditions (IMS) than in the one grown with NO_3^- (IMS+NO_3^-).

By applying high light to the non-diazotrophic filaments, we received the same response as we get naturally from diazotrophic filaments, i.e. cells with long fluorescence lifetime. The fact that high light increases fluorescence lifetime indicates that long lifetime is a stress response. Hence, the fact that cells under diazotrophic conditions have longer lifetime suggests that nitrogen fixers are more susceptible to

stress.

According to Berman-Frank et al. (2001b) N_2 fixation changes during the day and reaches its maximum during midday. For this reason, diel measurements were performed to see how the fluorescence lifetime of *Trichodesmium* varies at different times of the day. In diazotrophic IMS101, prolongation of the lifetime of PBS emission happened precisely at midday, thus, it corresponds to the peak of N_2 fixation. While the change is significant in the lifetimes of PBS, it is relatively small in chlorophyll, which is most easily explained by the disconnection of PBS. Conversely, the shortening of the PBS lifetime in non-diazotrophic IMS101 during midday can be attributed to an increase in photosynthesis. This is because the coupled PBS to PSII will transfer energy to chl-a, which will shorten its fluorescence lifetime, i.e. the energy from light is used for photosynthesis. Another possible explanation would be the appearance of something causing fluorescence quenching of PBS. Nevertheless, the noise of the data is high, thus, more replicates would be necessary to confirm these conclusions.

7.1.3 Fluorescence-Lifetime Imaging Microscopy

Overall, longer lifetime was observed in the nitrogen-fixing filaments. If we exclude the short filaments from the NO_3^--consuming samples, then the same applies to the first experiment. This implies more phycobilisomes uncoupling in the diazotrophic filaments, which is in line with the time-resolved fluorescence spectroscopy measurements.

The tips which often did not get stained are considered as a separate category type. One possible reason for not getting stained is that they are dying. This is most likely, especially in case the filaments result from breaking filaments. But in most cases they have probably a different function not related to N_2 fixation, they just happen to have lower activity both in N_2 and C fixation, the latter of which is behind the lack of Lugol staining.

The majority (90%) of the cells having a regular fluorescence lifetime are called "normal" as we assume that they are actively photosynthesising, which is in line with the full Lugol staining of these cells. According to the fluorescence lifetime spectroscopy measurements, this type of cells should have fluorescence lifetime of $\sim$70 or 140 ps, while using FLIM we observed lifetimes of $\sim$0.3 ns. These numbers do not match, most probably due to the instrument's response function of the Leica Stellaris microscope, which is about 0.2 ns.

The bright single cells with a significantly longer lifetime than in the neighbouring cells might be the so-called 'bright cells' according to Küpper et al. (2009). Although they appeared both in the first and second experiment, it was only 1-2 cells in 30 and 100 filaments, respectively, which is not even 1% of cells. If the average nitrogenase content per cell is 1.2 pg (based on a value of nifH per chl-a, Brown et al. (2008)) and average protein content in cell is 40 pg (based on the estimates of dry weight from other organisms and POC measurements on *Trichodesmium*, Eichner et al. (2014),Steinberg et al. (2002)), then 3% of total protein content is nitrogenase. This implies that if nitrogenase was the only protein in diazocyte cells, then 3% of all cells would have to be diazocytes. Although this estimate is a conservative estimate, this number is still larger than the number of diazocytes actually observed. Therefore, with this frequency of occurrence, we conclude that the bright single cells can not

be the only N_2-fixing cells, since they could not fit all the nitrogenase to supply the whole population of *Trichodesmium*. The same arguments apply also to the diazocyte-like bright segment observed since it appeared in 1/100 filaments only.

Additionally, we observed that not all the completely bright filaments appear unstained by Lugol's solution. It appears to depend on the length of the fluorescence lifetime. In Figure 6.20 the unstained parts correspond to the brighter parts, e.g. to the parts with longer fluorescence lifetime ($\sim$1.5 ns and higher). In Figure 6.23, there is a bright filament with $\sim$1 ns fluorescence lifetime which was fully stained. Based on these observations, one possible explanation is the different response rate of change of the fluorescence lifetime and Lugol staining to stress. If cells get stressed, the response in fluorescence lifetime can happen really fast, within seconds, for example by uncoupling of PBS. In contrast, the response in Lugol staining, which reflects the production of starch from CO_2, takes much longer, presumably in the order of hours. It is therefore very likely that the slightly longer lifetime of the filaments that are completely stained with Lugol's solution, would lengthen over time, and later, as the starch would be consumed over time, they would not get stained with Lugol's solution. Eventually, cell death could occur as observed in the time evolution experiment (Fig. 6.26).

Although there were no bright filaments observed in the non-diazotrophic samples, which could indicate a relationship with N_2 fixation mechanism, this behaviour is possibly caused by stress. This type of cells can be identified as the very bright cells introduced by H. Küpper (Kupper et al. (2004), Küpper et al. (2009)). The fact that no bright filaments appeared in the cultures grown with NO_3^- indicates a higher susceptibility of the nitrogen-fixing filaments to stress.

An unexpected phenomenon was the cell segments with short fluorescence lifetimes. A fast-FLIM picture carries information about the lifetime of fluorescence as well as its intensity. Thus, a possible explanation was that the dark blue segments appearing on the fast-FLIM pictures have a lower fluorescence intensity. This hypothesis can be rejected, as shown in Figure 7.4, where only the fluorescence intensity is the same throughout the image, especially in the marked section. Hence, the difference in fast -FLIM reflects an actual difference in lifetime.

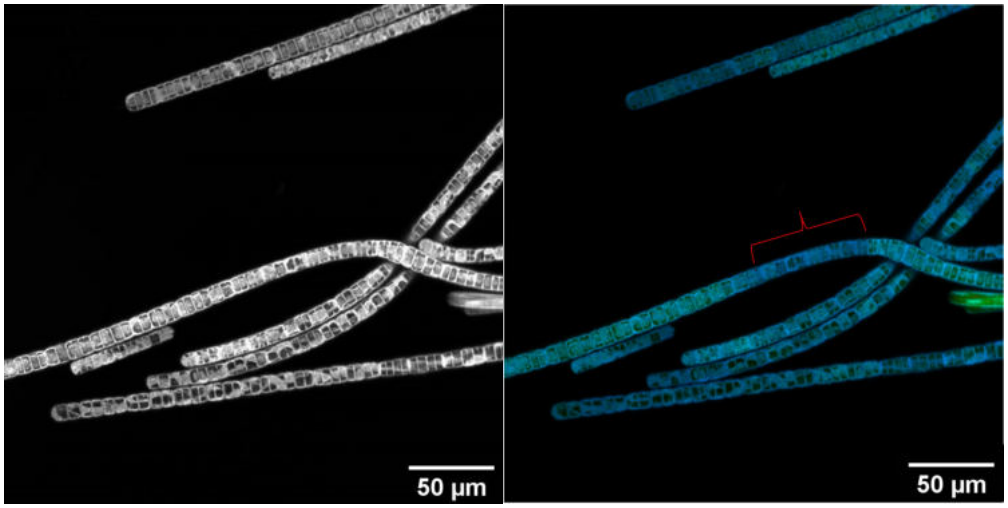

(a) Fluorescence intensity (b) Fast -FLIM

Figure 7.4: Comparison between the (a) fluorescence intensity image and (b) a fast -FLIM picture, showing both the fluorescence intensity and lifetime. The segment marked by a red line indicates the examined section with shorter lifetime.

Another possible hypothesis is that cells with short τ might have higher PSI:PSII ratio, since energy transfer in PSI is more efficient than in PSII (Nelson (2009)). This could support N_2-fixation by cyclic electron transport, leading to ATP production without concurrent O_2 production.

As for the morphology difference in width of the cells within the segments with short τ and the rest of the cells, the reason could be a lack of glycogen granules and gas vacuoles, resulting in a smaller cell size. Here we can refer to Sandh et al. (2012), who used TEM to look at the cellular ultrastructure of cells in the diazocyte zones, and claimed that "The most obvious adaptation was an extensive reduction in gas vacuole size and number, combined with a more condensed thylakoid network and, as evident from the Lugol staining, a reduced carbohydrate storage."

We consider the short bright filaments as a separate category type, because we believe that many of them result from the breaking of a long filament. This happens for example after death of a cell in the middle of a long filament, which we observed in the FLIM time evolution of fluorescence lifetime (Fig. 6.26). Hence, we attribute the long lifetime of the cells to stress and not to a potential N_2 fixation mechanism. This hypothesis is supported by the fact that the short bright filaments did not get stained by Lugol's solution.

In the time evolution of fluorescence lifetime experiment, we did not observe any switch from the long fluorescence lifetime back to the regular state, as expected based on Kupper et al. (2004) and Berman-Frank et al. (2001b). Both studies claimed that cells can turn photosynthetic activity on and off within 10 to 15 minutes. It is suggested that even the very bright cells, which is probably the case of cells in Figure 6.26, can switch to normal state in the range of 1 to 5 min. However, the only state change observed was the disappearance of cells. There is no evidence that the disappeared cells were unstained by Lugol's solution but we assume this based on the unstained surrounding cells. Dissolution of cells, long fluorescence lifetime and no Lugol staining indicate behaviour caused by stress.

7.2 *Trichodesmium* NIBB1067

Overall, for *Trichodesmium* NIBB1067 no significant difference between the filaments growing under diazotrophic and non-diazotrophic conditions was observed, except for more cells with higher fluorescence lifetime in the N_2-fixing filaments than in the NO_3^--using ones.

A morphological abnormality found in NIBB1067 but not IMS101 are the "granulated tips". These cells seem to be full of gas vacuoles. We do not know the reason of this, and it has not been described before (as far as we know).

7.2.1 Lugol staining

Given that an unstained segment was identified only in less than 2 % of filaments, which is not enough to supply the whole colony with nitrogen, there might be another reason for a lack of carbohydrates in these segments, not related to nitrogen fixation. The overall uneven staining pattern suggests that there is indeed some difference in the carbohydrate storage metabolism compared to the IMS101 strain. It is even possible that the N_2-fixing cells of NIBB1067 do have carbohydrates.

Moreover, the lack of unstained segments, indicating diazocytes, is in line with the nitrogenase proteins being located in almost all the cells (in > 95 % of total cells in this strain) (Taniuchi et al. (2008), Ohki (2008)).

7.2.2 Fluorescence-Lifetime Imaging Microscopy

In the first experiment, having observed more cells with long fluorescence lifetime in the NO_3^--consuming filaments than in the N_2-fixing ones, which is the opposite trend expected, was most likely caused by poor condition[1] of the filaments grown under non-diazotrophic treatment.

When omitting the filaments grown with NO_3^- from the first experiment, only a few cells with high (> 0.5 ns) fluorescence lifetime were observed. This indicates that the N_2 -fixing mechanism has to be other than the PBS uncoupling. Nevertheless, the fact that in the N_2-fixing filaments, there are more cells with long fluorescence lifetime might be attributed to higher susceptibility to stress, similar as in IMS101.

The short lifetime cells are again possibly a result of higher PSI:PSII ratio. The patchy pattern of these cells (visible in Fig. 6.14) could be a sign of nitrogenase being in an active form only in some cells although present in all of them. However, cells with short fluorescence lifetime appeared also in the filaments grown under non-diazotrophic conditions.

7.3 Comparison between IMS101 & NIBB1067

Prior to single cell level analyses, the bulk pigment composition the comparison of the PUB:PEB ratio in both strains, neglecting the addition of nitrate, showed a small but statistically-significant difference in pigment composition in *Trichodesmium* IMS101 and NIBB1067 which is consistent with the difference in the colour of the strains visible to the naked eye (see Fig. 7.5). This difference is small, however, it

[1] One day before performing the measurements, some filaments appeared greenish.

should be taken into account when comparing fluorescence spectra, although it will only have a minimal effect.

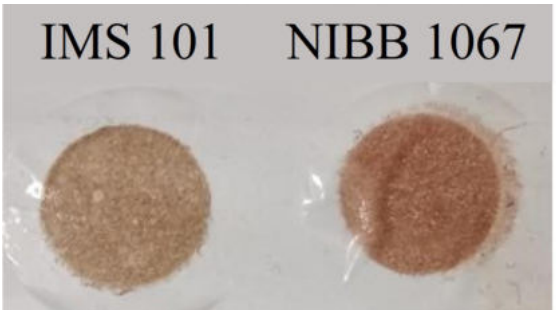

Figure 7.5: Comparison of filaments of *Trichodesmium* IMS101 and NIBB1067. There is a visible difference in the colour of the filaments, which indicates different pigments composition.

When considering the effect of added nitrate, the comparison of the strains did not show any statistically significant difference in phycobilisomes concentration between diazotrophic and non-diazotrophic filaments. Therefore, in subsequent observations of fluorescence spectra, any differences in intensity and frequency of occurrence of bright cells will be attributed to energy flow (uncoupling of PBS).

All the p-values proving a statistically significant difference in PUB:PEB ratios were smaller than the chosen significance level $\alpha = 0.05$, but not by much. In the comparison of IMS101 and NIBB1067, it was $p = 0.005$ and in the comparison of the strains under both diazotrophic and non-diazotrophic conditions, where the difference was proven between non-diazotrophic NIBB1067 and diazotrophic IMS it was $p = 0.0406$. Because of the low number of samples, there is a high risk of type 1 error, especially in multiple comparisons.

Overall, the strains IMS101 and NIBB1067 show different patterns, both in Lugol staining and fluorescent lifetime of the cells. The main differences are summarised in Table 7.1.

	IMS101		NIBB1067	
Condition	N_2	NO_3^-	N_2	NO_3^-
PUB:PEB	a	ab	ab	b
Lugol	Unstained seg.	Fully stained	Fully stained	Fully stained
	Homogenous staining		Uneven staining	
FLIM	Long τ	Regular τ	$\pm$ regular τ	Regular τ
	Short τ seg.	Short τ seg.	Short τ seg.	Short τ seg.
Fl. τ spectr.	More free PBS	Less free PBS	-	-
Other			Granulated tips	

Table 7.1: Comparison between all the measured and observed properties of *Trichodesmium* IMS101 and NIBB1067. Both for diazotrophic (N_2) and non-diazotrophic (NO_3^-) conditions. The letters *a* and *b* in the PUB:PEB comparison indicate which groups are significantly different, i.e. the ratio differs between the strains in general but when comparing all the groups separately, it differs only between the N_2-fixing IMS101 and NO_3^--consuming NIBB1067. The PUB:PEB ratio was higher for NIBB1067 (i.e. a<b).

As mentioned previously, the Lugol staining pattern in IMS101 cells is homogeneous and the occurrence of unstained segments, considered as diazocytes, is nearly the same among the filaments, i.e. there is one diazocyte per filament and it appears approximately at the middle of the filament. In contrast, the cells of NIBB1067 did not get fully stained (when using the same concentration of Lugol's solution as for staining IMS101) and the occurrence of completely unstained cells was rare. This is evidenced in Figure 6.25. The most likely explanation for this observation is a different carbohydrate storage metabolism.

Similar patterns as in Lugol staining were observed in FLIM images. While the filaments of IMS101 appear homogeneous, except for the bright filaments/cells and short lifetime segments, the filaments of NIBB1067 appear patchy due to the uneven distribution of the short lifetime cells. This might be caused by different distribution of nitrogenase in the filaments of IMS101 and NIBB1067.

Finally, a common feature is apparently a greater susceptibility to stress in the cells grown under diazotrophic conditions. However, due to the higher frequency of cells with long fluorescence lifetime, it can be concluded that IMS101 is more susceptible to stress than NIBB1067.

Conclusion

The main task of this thesis was to study photophysiological characteristics related to the hypothesis about PBS uncoupling enabling N_2 fixation introduced by Küpper et al. (2009) and compare the findings between two strains of *Trichodesmium* IMS101 and NIBB1067. In order to achieve this, fluorescence lifetime measurements were performed. First, at bulk level, using Time-resolved fluorescence spectroscopy, and second, at single-cell resolution, using Fluorescence-lifetime imaging microscopy (FLIM). Combination of FLIM with Lugol's stain allowed us to directly relate fluorescence lifetime patterns to staining patterns of a commonly used marker of N_2 fixing cells. Cultures of both strains were cultivated both in diazotrophic and non-diazotrophic conditions, to ensure the relation of the results with N_2 fixation.

For the IMS101 strain, time-resolved fluorescence spectroscopy revealed four components in the fluorescence decay. Two components were in order of ps and were attributed to energy transfer from PBS to chl-a and energy trapping within PSII. The other two, in order of ns, were ascribed to uncoupled PBS. Furthermore, it was shown that in the N_2-fixing culture the relative amount of PBS that does not transfer energy is about two times higher than in the NO_3-supplied culture. By application of high-light on the non-diazotrophic filaments, we found that high light and diazotrophy have a similar effect, both causing elevated fluorescence lifetime. This indicates that long fluorescence lifetime reflects a stress response. The fact that there are more filaments with long lifetime in N_2 fixers suggests that they are more susceptible to stress. Measurements for the NIBB1067 strain have not been performed yet and need to be done in future.

In the FLIM measurements of IMS101, seven different types of patterns were identified. One of them, the so-called bright cell introduced by Küpper et al. (2009) was observed only once. With this frequency of occurrence, we conclude that the bright single cells can not be the only N2-fixing cells, since they could not fit all the nitrogenase to supply the whole population of *Trichodesmium*. However, an unexpected phenomenon, cell segments with short fluorescence lifetime corresponding to diazocyte-like segments unstained by Lugol's solution, was observed. A possible explanation could be higher PSI:PSII ratio in these cells. This could support N_2 fixation by cyclic electron transport leading to ATP production without concurrent O_2 production. This can be tested in future with a PSI antibody or mRNA FISH probe.

In The FLIM measurements of NIBB1067 almost no cells with long fluorescence lifetime were observed. However, there were many cells with short fluorescence lifetime and they seem to be randomly distributed along the filaments. This "patchy" pattern resembles the Lugol staining patterns which were not as homogeneous as in IMS101.

In conclusion, the strains IMS101 and NIBB1067 showed different patterns both in Lugol and fluorescence lifetime patterns, which indicates different N_2 fixing mechanisms in each of them. The elevated fluorescence lifetime in the filaments grown under N_2 fixing conditions of both strains is most probably indicating a greater susceptibility to stress rather than a direct N_2 fixing mechanism, hence, our findings are not in agreement with the hypothesis proposed by Küpper et al. (2009). Overall, the study highlights the intricate interplay of photosynthetic electron flow with

N2 fixation at single-cell level in *Trichodesmium* and calls for a re-evaluation of the current understanding of nitrogenase protection by regulation of photosynthesis.

Bibliography

Acuña, A. M., Lemaire, C., van Grondelle, R., Robert, B., and van Stokkum, I. H. (2018). Energy transfer and trapping in *Synechococcus* WH 7803. *Photosynthesis research*, 135(1):115–124.

aquaportail (2020). Phycobilisome: définition. `https://www.aquaportail.com/definition-1316-phycobilisome.html`.

Arrigo, K. R. (2005). Marine microorganisms and global nutrient cycles. *Nature*, 437(7057):349–355.

Atkins, P. W. and Friedman, R. S. (2011). *Molecular quantum mechanics*. Oxford university press.

Bailey, J. and Whelan, W. (1961). Physical properties of starch. *J. biol. Chem*, 236(4):969–73.

Bergman, B. and Carpenter, E. J. (1991). Nitrogenase confined to randomly distributed trichomes in the marine cyanobacterium *Trichodesmium thiebauthii* 1. *Journal of Phycology*, 27(2):158–165.

Berman-Frank, I., Cullen, J. T., Shaked, Y., Sherrell, R. M., and Falkowski, P. G. (2001a). Iron availability, cellular iron quotas, and nitrogen fixation in *Trichodesmium*. *Limnology and Oceanography*, 46(6):1249–1260.

Berman-Frank, I., Lundgren, P., Chen, Y.-B., Kupper, H., Kolber, Z., Bergman, B., and Falkowski, P. (2001b). Segregation of nitrogen fixation and oxygenic photosynthesis in the marine cyanobacterium *Trichodesmium*. *science*, 294(5546):1534–1537.

Berman-Frank, I., Lundgren, P., and Falkowski, P. (2003). Nitrogen fixation and photosynthetic oxygen evolution in cyanobacteria. *Research in microbiology*, 154(3):157–164.

Blankenship, R. E. (2021). *Molecular mechanisms of photosynthesis*. John Wiley & Sons.

Brown, C. M., MacKinnon, J. D., Cockshutt, A. M., Villareal, T. A., and Campbell, D. A. (2008). Flux capacities and acclimation costs in *Trichodesmium* from the Gulf of Mexico. *Marine Biology*, 154(3):413–422.

Bücherl, C. A., Bader, A., Westphal, A. H., Laptenok, S. P., and Borst, J. W. (2014). FRET-FLIM applications in plant systems. *Protoplasma*, 251(2):383–394.

Bulen, W. and LeComte, J. (1966). The nitrogenase system from *Azotobacter*: two-enzyme requirement for N_2 reduction, ATP-dependent H_2 evolution, and ATP hydrolysis. *Proceedings of the National Academy of Sciences*, 56(3):979–986.

Burgess, B. K. and Lowe, D. J. (1996). Mechanism of molybdenum nitrogenase. *Chemical reviews*, 96(7):2983–3012.

Campbell, N., Reece, J., and Mitchell, L. (1996). Biology 5th edition Benjamin Cummings. *Campion, D., C. Dumanchin, etal.(1999)." Early onset autosomal dominant Alzheimer disease: prevalence, geneticheterogeneity, and mutation spectrum." AmJHumGenet65 (3)*, 66470.

Capone, D. G., Zehr, J. P., Paerl, H. W., Bergman, B., and Carpenter, E. J. (1997). *Trichodesmium*, a globally significant marine cyanobacterium. *Science*, 276(5316):1221–1229.

Chen, Y.-B., Dominic, B., Zani, S., Mellon, M. T., and Zehr, J. P. (1999). Expression of photosynthesis genes in relation to nitrogen fixation in the diazotrophic filamentous nonheterocystous cyanobacterium *Trichodesmium* sp. IMS 101. *Plant molecular biology*, 41(1):89–104.

Chen, Y.-B., Zehr, J. P., and Mellon, M. (1996). Growth and nitrogen fixation of the diazotrophic filamentous nonheterocystous cyanobacterium *Trichodesmium* sp. IMS101 in defined media: evidence for a circadian rhythm 1. *Journal of Phycology*, 32(6):916–923.

Cohen-Bazire, G., Pfennig, N., and Kunisawa, R. (1964). The fine structure of green bacteria. *The Journal of cell biology*, 22(1):207–225.

Collos, Y., Mornet, F., Sciandra, A., Waser, N., Larson, A., and Harrison, P. (1999). An optical method for the rapid measurement of micromolar concentrations of nitrate in marine phytoplankton cultures. *Journal of Applied Phycology*, 11(2):179–184.

De Mandal, S., Laskar, F., Panda, A. K., and Mishra, R. (2020). Microbial diversity and functional potential in wetland ecosystems. In *Recent Advancements in Microbial Diversity*, pages 289–314. Elsevier.

Dixon, R. and Kahn, D. (2004). Genetic regulation of biological nitrogen fixation. *Nature Reviews Microbiology*, 2(8):621–631.

Durner, J., Böhm, I., Knörzer, O., and Böger, P. (1996). Proteolytic degradation of dinitrogenase reductase from *Anabaena variabilis* (ATCC 29413) as a consequence of ATP depletion and impact of oxygen. *Journal of bacteriology*, 178(3):606–610.

Edinburch Instruments (2022). What is a Jablonski diagram (Perrin-Jablonski diagram)? `https://www.edinst.com/us/blog/jablonski-diagram/`.

Ehrenberg, C. (1830). Neue Beobachlungen über blutartige Erscheinungen in Aegypten, Arabien und Sibirien, nebst einer Uebersicht und Kritik der früher bekannnten. *Annalen der Physik*, 94(4):477–514.

Eichner, M., Kranz, S. A., and Rost, B. (2014). Combined effects of different CO_2 levels and N sources on the diazotrophic cyanobacterium *Trichodesmium*. *Physiologia plantarum*, 152(2):316–330.

Encyclopedia Britannica (1998). The patway of electrons. `https://www.britannica.com/science/photosynthesis/The-pathway-of-electrons#/media/1/458172/3105`.

Fredriksson, C. and Bergman, B. (1995). Nitrogenase quantity varies diurnally in a subset of cells within colonies of the non-heterocystous cyanobacteria *Trichodesmium* spp. *Microbiology*, 141(10):2471–2478.

Fredriksson, C. and Bergman, B. (1997). Ultrastructural characterisation of cells specialised for nitrogen fixation in a non-heterocystous cyanobacterium, *Trichodesmium* spp. *Protoplasma*, 197(1):76–85.

Fujita, Y. and Shimura, S. (1974). Phycoerythrin of the marine blue-green alga *Trichodesmium thiebautii*. *Plant and cell physiology*, 15(5):939–942.

Gallon, J. (1992). Tansley review no. 44. reconciling the incompatible: N_2 fixation and O_2. *New Phytologist*, pages 571–609.

Galloway, J. N., Townsend, A. R., Erisman, J. W., Bekunda, M., Cai, Z., Freney, J. R., Martinelli, L. A., Seitzinger, S. P., and Sutton, M. A. (2008). Transformation of the nitrogen cycle: recent trends, questions, and potential solutions. *Science*, 320(5878):889–892.

Gao, H., Matyka, M., Liu, B., Khalili, A., Kostka, J. E., Collins, G., Jansen, S., Holtappels, M., Jensen, M. M., Badewien, T. H., et al. (2012). Intensive and extensive nitrogen loss from intertidal permeable sediments of the Wadden Sea. *Limnology and Oceanography*, 57(1):185–198.

Giblin, A. E., Tobias, C. R., Song, B., Weston, N., Banta, G. T., and H. RIVERA-MONROY, V. (2013). The importance of dissimilatory nitrate reduction to ammonium (DNRA) in the nitrogen cycle of coastal ecosystems. *Oceanography*, 26(3):124–131.

Gilbert, A. and Baggott, J. E. (1991). *Essentials of molecular photochemistry*.

Grabowski, J. and Gantt, E. (1978). Photophysical properties of phycobiliproteins from phycobilisomes: fluorescence lifetimes, quantum yields, and polarization spectra. *Photochemistry and photobiology*, 28(1):39–45.

Green, B., Parson, W. W., and Parson, W. W. (2003). *Light-harvesting antennas in photosynthesis*, volume 13. Springer Science & Business Media.

Gruber, N. (2008). The marine nitrogen cycle: overview and challenges. *Nitrogen in the marine environment*, 2:1–50.

Hamilton, T. L., Boyd, E. S., and Peters, J. W. (2011). Environmental constraints underpin the distribution and phylogenetic diversity of nifh in the Yellowstone geothermal complex. *Microbial ecology*, 61(4):860–870.

Haselkorn, R. (1978). Heterocysts. *Annual Review of Plant Physiology*, 29(1):319–344.

Hoffman, B. M., Lukoyanov, D., Yang, Z.-Y., Dean, D. R., and Seefeldt, L. C. (2014). Mechanism of nitrogen fixation by nitrogenase: the next stage. *Chemical reviews*, 114(8):4041–4062.

Holland, H. D. (1997). Evidence for life on Earth more than 3850 million years ago. *Science*, 275(5296):38–39.

Hynes, A. M., Webb, E. A., Doney, S. C., and Waterbury, J. B. (2012). Comparison of cultured *Trichodesmium* (Cyanophyceae) with species characterized from the field 1. *Journal of phycology*, 48(1):196–210.

Jain, A., Blum, C., and Subramaniam, V. (2009). Chapter 4 - fluorescence lifetime spectroscopy and imaging of visible fluorescent proteins. In Verdonck, P., editor, *Advances in Biomedical Engineering*, pages 147–176. Elsevier, Amsterdam.

Janaki, S. and Wolk, C. P. (1982). Synthesis of nitrogenase by isolated heterocysts. *Biochimica et Biophysica Acta (BBA)-Gene Structure and Expression*, 696(2):187–192.

Karl, D. M. and Michaels, A. F. (2001). Nitrogen cycle. *Encylopedia of Ocean Science*, pages 1876–1884.

Koirala, A. and Brözel, V. S. (2021). Phylogeny of nitrogenase structural and assembly components reveals new insights into the origin and distribution of nitrogen fixation across bacteria and archaea. *Microorganisms*, 9(8):1662.

Kolter, R. (2022). Diazomonia ii - *Trichodesmium*. `https://schaechter.asmblog.org/schaechter/2022/02/diazomania-ii-trichodesmium.html`.

Küpper, H., Andresen, E., Wiegert, S., Šimek, M., Leitenmaier, B., and Šetlík, I. (2009). Reversible coupling of individual phycobiliprotein isoforms during state transitions in the cyanobacterium *Trichodesmium* analysed by single-cell fluorescence kinetic measurements. *Biochimica et Biophysica Acta (BBA)-Bioenergetics*, 1787(3):155–167.

Kupper, H., Ferimazova, N., Setlik, I., and Berman-Frank, I. (2004). Traffic lights in *Trichodesmium*. Regulation of photosynthesis for nitrogen fixation studied by chlorophyll fluorescence kinetic microscopy. *Plant physiology*, 135(4):2120–2133.

Küpper, H., Šetlík, I., Trtílek, M., and Nedbal, L. (2000). A microscope for two-dimensional measurements of in vivo chlorophyll fluorescence kinetics using pulsed measuring radiation, continuous actinic radiation, and saturating flashes. *Photosynthetica*, 38(4):553–570.

Kwiatkowski, L., Aumont, O., Bopp, L., and Ciais, P. (2018). The impact of variable phytoplankton stoichiometry on projections of primary production, food quality, and carbon uptake in the global ocean. *Global Biogeochemical Cycles*, 32(4):516–528.

Lakowicz, J. R. (1999). *Introduction to Fluorescence*, pages 1–23. Springer US, Boston, MA.

Legendre, L., Rivkin, R., Weinbauer, M., Guidi, L., and Uitz, J. (2015). The microbial carbon pump concept: Potential biogeochemical significance in the globally changing ocean. *Progress in Oceanography*, 134.

Leigh, G. J. (2002). *Nitrogen fixation at the millennium*. Elsevier.

Li, Y., Natakorn, S., Chen, Y., Safar, M., Cunningham, M., Tian, J., and Li, D. D.-U. (2020). Investigations on average fluorescence lifetimes for visualizing multi-exponential decays. *Frontiers in Physics*, 8.

Loefroth, J. E. (1986). Time-resolved emission spectra, decay-associated spectra, and species-associated spectra. *The Journal of Physical Chemistry*, 90(6):1160–1168.

Luis, A., Bernd, W., Bram, v. d. B., Giulia, O., Kees, J., Lioba, K., Julia, R., and Frank, H. (2019). A novel concept in fluorescence lifetime imaging enabling video-rate confocal FLIM. https://www.leica-microsystems.com/science-lab/a-novel-concept-in-fluorescence-lifetime-imaging-enabling-video -rate-confocal-flim/.

Mahaffey, C., Michaels, A. F., and Capone, D. G. (2005). The conundrum of marine N_2 fixation. *American Journal of Science*, 305(6-8):546–595.

Marcu, L., French, P. M., and Elson, D. S. (2014). *Fluorescence lifetime spectroscopy and imaging: principles and applications in biomedical diagnostics*. CRC Press.

Masojídek, J., Torzillo, G., and Koblížek, M. (2013). Photosynthesis in microalgae. *Handbook of microalgal culture: applied phycology and biotechnology*, pages 21–36.

MCB, H. (2007). The dark reactions of photosynthesis generate sugar from carbon dioxide. `https://www.labxchange.org/library/pathway/lx-pathway:21ad31e3-402a-48ce-89c6-159a03ec2cd5/items/lx-pb:21ad31e3-402a-48ce-89c6-159a03ec2cd5:html:5ad2a03a`.

Millar, D. P. (1996). Time-resolved fluorescence spectroscopy. *Current opinion in structural biology*, 6(5):637–642.

Mulholland, M. R., Bronk, D. A., and Capone, D. G. (2004). Dinitrogen fixation and release of ammonium and dissolved organic nitrogen by *Trichodesmium* IMS101. *Aquatic Microbial Ecology*, 37(1):85–94.

Mulholland, M. R. and Capone, D. G. (2009). Dinitrogen fixation in the Indian Ocean. *Washington DC American Geophysical Union Geophysical Monograph Series*, 185:167–186.

Nelson, N. (2009). Plant photosystem i–the most efficient nano-photochemical machine. *Journal of nanoscience and nanotechnology*, 9(3):1709–1713.

Nelson, N. and Yocum, C. F. (2006). Structure and function of photosystems i and ii. *Annu. Rev. Plant Biol.*, 57:521–565.

O'Connor, D. (2012). *Time-correlated single photon counting*. Academic press.

Ohki, K. (2008). Intercellular localization of nitrogenase in a non-heterocystous cyanobacterium (Cyanophyte), *Trichodesmium* sp. NIBB1067. *Journal of oceanography*, 64(2):211–216.

Ohki, K. and Fujita, Y. (1982). Laboratory culture of the pelagic blue-green alga *Trichodesmium thiebautii*: conditions for unialgal culture. *Mar. Ecol. Prog. Ser*, 7:185–190.

Ohki, K., Zehr, J. P., Falkowski, P. G., and Fujita, Y. (1991). Regulation of nitrogen-fixation by different nitrogen sources in the marine non-heterocystous cyanobacterium *Trichodesmium* sp. NIBB1067. *Archives of microbiology*, 156(5):335–337.

Paerl, H. W. and Bebout, B. M. (1988). Direct measurement of O_2-depleted microzones in marine *Oscillatoria*: relation to N_2 fixation. *Science*, 241(4864):442–445.

Peter, M., Ameer-Beg, S. M., Hughes, M. K., Keppler, M. D., Prag, S., Marsh, M., Vojnovic, B., and Ng, T. (2005). Multiphoton-FLIM quantification of the EGFP-mRFP1 FRET pair for localization of membrane receptor-kinase interactions. *Biophysical journal*, 88(2):1224–1237.

Pi, H.-W., Lin, J.-J., Chen, C.-A., Wang, P.-H., Chiang, Y.-R., Huang, C.-C., Young, C.-C., and Li, W.-H. (2022). Origin and evolution of nitrogen fixation in prokaryotes. *Molecular biology and evolution*, 39(9):msac181.

Postgate, J. (1998). *Nitrogen fixation*. Cambridge University Press.

Protocols, C. S. H. (2007). PBS (10x) without potassium salt. `http://cshprotocols.cshlp.org/content/2007/4/pdb.rec10917.full?text_only=true`.

Prufert-Bebout, L., Paerl, H. W., and Lassen, C. (1993). Growth, nitrogen fixation, and spectral attenuation in cultivated *Trichodesmium* species. *Applied and Environmental Microbiology*, 59(5):1367–1375.

Raymond, J., Siefert, J. L., Staples, C. R., and Blankenship, R. E. (2004). The Natural History of Nitrogen Fixation. *Molecular Biology and Evolution*, 21(3):541–554.

Rippka, R., Waterbury, J., and Cohen-Bazire, G. (1974). A cyanobacterium which lacks thylakoids. *Archives of microbiology*, 100(1):419–436.

Ruben, S., Randall, M., Kamen, M., and Hyde, J. L. (1941). Heavy oxygen (o18) as a tracer in the study of photosynthesis. *Journal of the American Chemical Society*, 63(3):877–879.

Rysgaard, S., Glud, R. N., Risgaard-Petersen, N., and Dalsgaard, T. (2004). Denitrification and anammox activity in Arctic marine sediments. *Limnology and oceanography*, 49(5):1493–1502.

Sandh, G., El-Shehawy, R., Díez, B., and Bergman, B. (2009). Temporal separation of cell division and diazotrophy in the marine diazotrophic cyanobacterium *Trichodesmium* erythraeum IMS101. *FEMS Microbiology Letters*, 295(2):281–288.

Sandh, G., Ran, L., Xu, L., Sundqvist, G., Bulone, V., and Bergman, B. (2011). Comparative proteomic profiles of the marine cyanobacterium *Trichodesmium* erythraeum IMS101 under different nitrogen regimes. *Proteomics*, 11(3):406–419.

Sandh, G., Xu, L., and Bergman, B. (2012). Diazocyte development in the marine diazotrophic cyanobacterium *Trichodesmium*. *Microbiology*, 158(2):345–352.

Schlesinger, W. H. and Bernhardt, E. S. (2013). *Biogeochemistry: an analysis of global change*. Academic press.

Seefeldt, L. C., Yang, Z.-Y., Lukoyanov, D. A., Harris, D. F., Dean, D. R., Raugei, S., and Hoffman, B. M. (2020). Reduction of substrates by nitrogenases. *Chemical reviews*, 120(12):5082–5106.

Shively, J., Cannon, G., Heinhorst, S., Fuerst, J., Bryant, D., Gantt, E., Maupin-Furlow, J., Schüler, D., Pfeifer, F., Docampo, R., Dahl, C., Preiss, J., Steinbüchel, A., and Federici, B. (2009). Intracellular structures of prokaryotes: Inclusions, compartments and assemblages. In Schaechter, M., editor, *Encyclopedia of Microbiology (Third Edition)*, pages 404–424. Academic Press, Oxford, third edition edition.

Steinberg, D. K., Goldthwait, S. A., and Hansell, D. A. (2002). Zooplankton vertical migration and the active transport of dissolved organic and inorganic nitrogen in the Sargasso Sea. *Deep Sea Research Part I: Oceanographic Research Papers*, 49(8):1445–1461.

Sukenik, A., Zohary, T., and Padisák, J. (2009). Cyanoprokaryota and other prokaryotic algae. In Likens, G. E., editor, *Encyclopedia of Inland Waters*, pages 138–148. Academic Press, Oxford.

Taiz, L. and Zeiger, E. (2002). *Plant Physiology, 3rd ed.* Sinauer Associates.

Taniuchi, Y., Murakami, A., and Ohki, K. (2008). Whole-cell immunocytochemical detection of nitrogenase in cyanobacteria: improved protocol for highly fluorescent cells. *Aquatic microbial ecology*, 51(3):237–247.

Van Niel, C., Ruben, S., Carson, S., Kamen, M., and Foster, J. (1942). Radioactive carbon as an indicator of carbon dioxide utilization: VIII. the role of carbon dioxide in cellular metabolism. *Proceedings of the National Academy of Sciences*, 28(1):8–15.

Volk, T. and Hoffert, M. I. (1985). Ocean carbon pumps: Analysis of relative strengths and efficiencies in ocean-driven atmospheric CO_2 changes. *The carbon cycle and atmospheric CO_2: natural variations Archean to present*, 32:99–110.

Waterbury, J. B. (1986). Biological and ecological characterization of the marine unicellular cyanobacterium *Synechococcus*. *Photosynthetic picoplankton*, pages 71–120.

Weiss, M. C., Sousa, F. L., Mrnjavac, N., Neukirchen, S., Roettger, M., Nelson-Sathi, S., and Martin, W. F. (2016). The physiology and habitat of the last universal common ancestor. *Nature microbiology*, 1(9):1–8.

Zehr, J. P. and Capone, G. D. (2021). *Marine Nitrogen Fixation*. Springer Nature Switzerland AG.

Zehr, J. P. and Ward, B. B. (2002). Nitrogen cycling in the ocean: new perspectives on processes and paradigms. *Applied and environmental microbiology*, 68(3):1015–1024.

List of Abbreviations

anammox	anaerobic ammonia oxidation
APC	allophycocyanin
ATP	adenosine triphosphate
BNF	biological nitrogen fixation
DAS	Decay-Associated Spectra
DIC	dissolved inorganic carbon
DNRA	dissimilatory nitrate reduction to ammonium
DON	dissolved organic nitrogen
F_0	basic fluorescence yield of the dark-adapted state
F_m	maximal fluorescence yield of the dark-adapted state
F_v	variable fluorescence
FLIM	Fluorescence-Lifetime Imaging Microscopy
IRF	instrument response function
LUCA	last universal common ancestor
N_2	dinitrogen gas
NADPH	nicotine adenine dinucleotide phosphate
PBS	phycobilisom
PC	phycocyanin
PE	phycoerythrin
PEB	phycoerythrobilin
PON	particulate organic nitrogen
PS	photosystem
PUB	phycourobilin
RC	reaction centre
TCSPC	Time-Correlated Single Photon Counting

A. Attachments

A.1 Comparison between fluorescence and Lugol staining patterns

The rest of the pictures from FLIM measurement of *Trichodesmium* IMS101 grown under N_2 fixing conditions compared to Lugol staining patterns. Red lines indicate special cell type (as described in Table 6.1), and the arrows indicate filaments in the Lugol staining picture corresponding to the bright filaments in fast-FLIM pictures. The colour scale ranges from 0 to 2 ns.

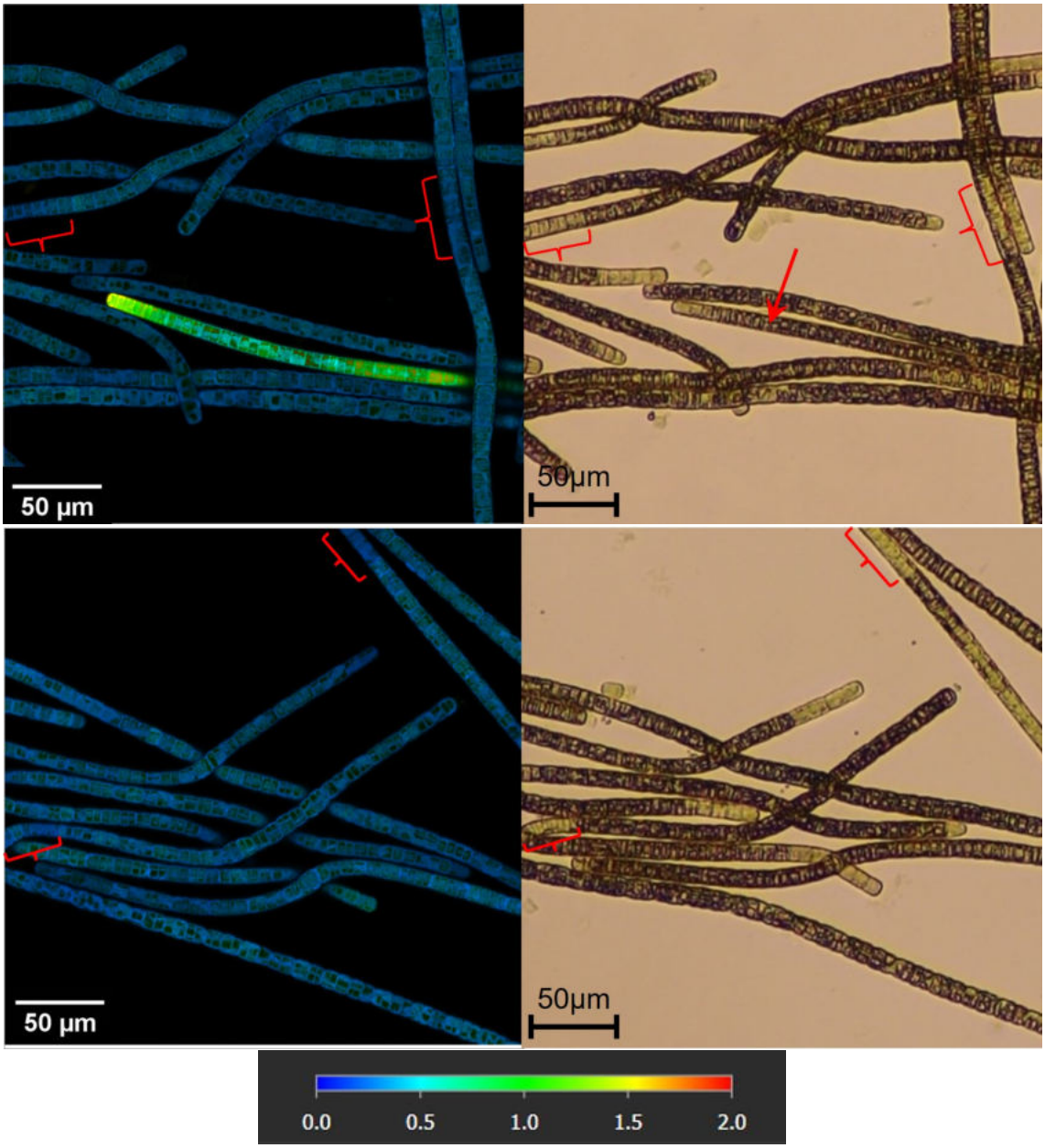

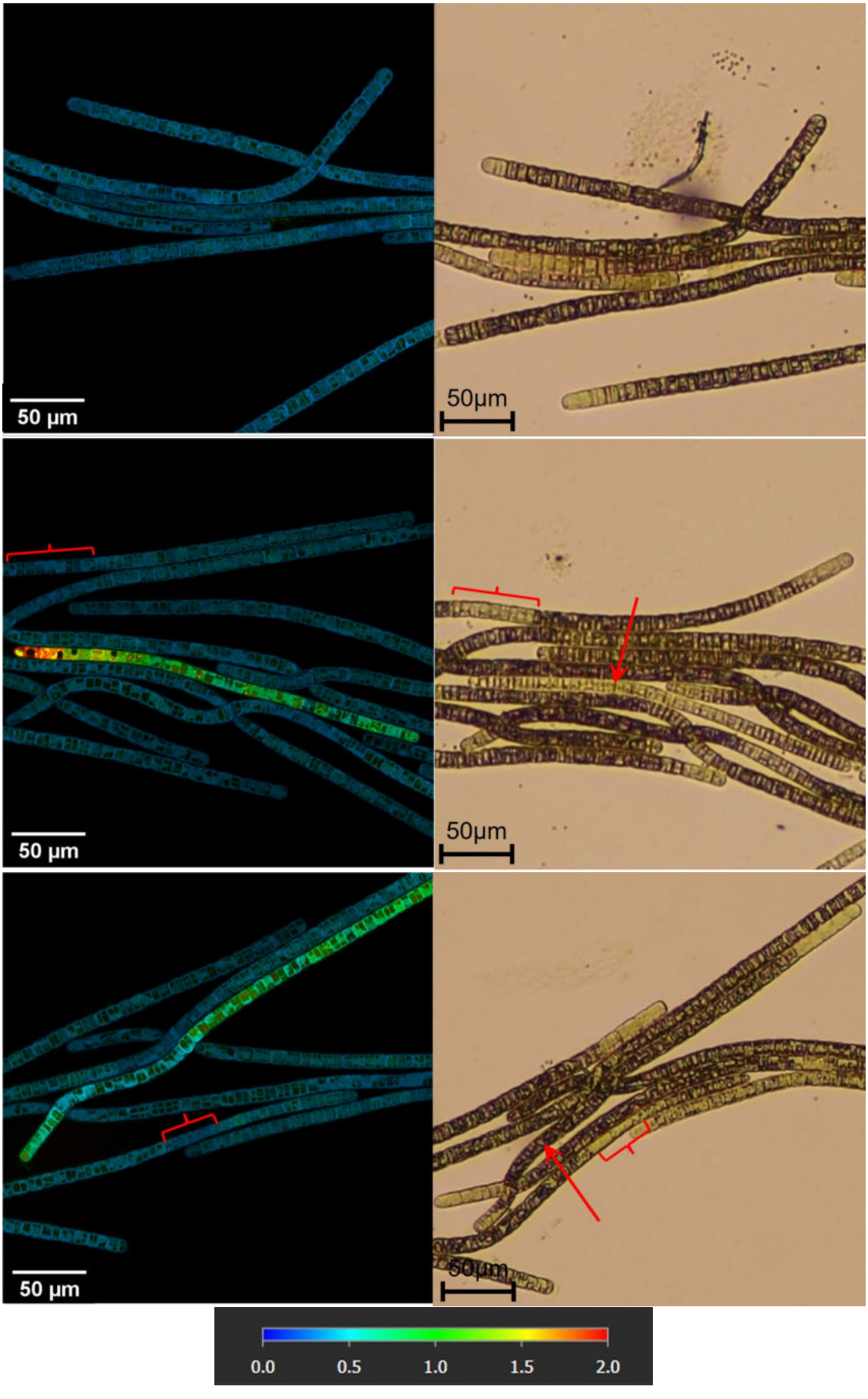
50 µm
50µm
50 µm
50µm
50 µm
50µm
0.0
0.5
1.0
1.5
2.0